Antigen retrieval and clearing for whole organ immunofluorescence by FLASH

Hendrik A. Messal[1,2,8], Jorge Almagro[1,8], May Zaw Thin[1], Antonio Tedeschi[1], Alessandro Ciccarelli[3], Laura Blackie[4], Kurt I. Anderson[3], Irene Miguel-Aliaga[4], Jacco van Rheenen[2], Axel Behrens[1,5,6,7*]

[1]Adult Stem Cell Laboratory, The Francis Crick Institute, 1 Midland Road, London NW1 1AT, UK

[2]Department of Molecular Pathology, Oncode Institute, Netherlands Cancer Institute, 1066 CX Amsterdam, the Netherlands

[3]Advanced Light Microscopy Facility, The Francis Crick Institute, 1 Midland Road, London NW1 1AT, UK

[4]MRC London Institute of Medical Sciences, Imperial College London, Hammersmith Campus, Du Cane Road, London W12 0NN, UK

[5]King's College London, Faculty of Life Sciences and Medicine, Guy's Campus, London SE121 1UL, UK

[6]Convergence Science Centre, Imperial College London, South Kensington Campus, London SW7 2AZ

[7]The Institute of Cancer Research, 237 Fulham Road, London SW3 6JB

[8]Equal contribution

*Corresponding author; e-mail: axel.behrens@crick.ac.uk

KEYWORDS: FLASH, 3D, clearing, immunofluorescence, light-sheet fluorescent microscopy, confocal microscopy, organ, epithelia, cancer, embryo

EDITORIAL SUMMARY This protocol describes how to perform antigen retrieval and tissue clearing for volumetric imaging of whole organs, organoids and small organisms using FLASH (Fast Light-microscopic analysis of Antibody-Stained wHole organs).

TWEET A new protocol for tissue clearing and immunostaining of whole organs, organoids and small organisms #FLASH @behrens_lab

COVER TEASER 3D immunofluorescence of intact organs by FLASH

ABSTRACT

Advances in light-sheet and confocal microscopy now allow imaging of cleared large biological tissue samples and enable the three-dimensional appreciation of cell and protein localization in their native organ environment. However, the sample

preparations for such imaging are often onerous and their capability for antigen detection limited. Here we describe FLASH (Fast Light-microscopic analysis of Antibody-Stained wHole organs), a simple and rapid, fully customizable technique for molecular phenotyping of intact tissue volumes. FLASH utilizes non-degradative epitope recovery and membrane solubilisation to enable the detection of a multitude of membranous, cytoplasmic and nuclear antigens in whole mouse organs and embryos, human biopsies, organoids and *Drosophila*. Retrieval and immunolabelling of epithelial markers, an obstacle for previous clearing techniques, can be achieved with FLASH. Upon volumetric imaging, FLASH-processed samples preserve their architecture and integrity, and can be paraffin-embedded for subsequent histopathological analysis. The technique can be performed by scientists trained in light microscopy and yields results in less than one week.

Introduction

The three-dimensional analysis of intact biological specimens unlocks answers to a wide range of research problems, such as the unbiased localization of rare cell types and quantitative insights into cell-tissue architectural relationships, cellular networks, morphological alterations and subcellular structures. This wealth of information comes at the cost of complex requirements for sample processing, imaging, data storage and interpretation, which are met by a range of recent technical developments, summarized below. Here, we describe a detailed protocol for FLASH (Fast Light-microscopic analysis of Antibody-Stained wHole organs)[1,2], a versatile approach for whole organ molecular labelling and clarification that enables high-resolution immunofluorescence in 3D for a broad range of samples (Fig. 1).

Advances in volumetric imaging and analysis

Since the development of selective plane illumination microscopy (SPIM)[3], 3D imaging of large samples such as whole organs and even entire organisms has flourished[4,5]. Clearing methods have been developed for imaging of organoids[6-8], organs expressing endogenous fluorophores[9-15], whole mice[16-18] and human organs[19], to overcome their opacity and scattering properties. Recently, ultrathin structured (lattice) light-sheet microscopy has allowed super-resolution imaging of

molecules and cells during embryogenesis[20]. These possibilities in 3D imaging with diverse magnifications, from molecules to organisms, call for potent computational techniques that allow maximum data mining. The era of machine learning brings promise to the analysis of large multidimensional datasets with expert-human accuracy[21,22]. Incipient pipelines for analysis of large-scale imaging data have been developed for inferring super-resolution in confocal images[23], quantifying metastases in entire mice[18] or mapping the mouse brain vasculature with unprecedented detail[24]. To fully exploit these advances, we need to be able to apply 3D imaging to the widest possible variety of specimens and molecules of interest.

Considerations on sample processing

Three-dimensional molecular tissue phenotyping requires that an organ is both optically transparent, to allow light-microscopic analysis, and accessible to antibodies, to enable cell and tissue identification by immunolabelling[5]. Over the last decade, several techniques have been developed to enhance tissue transparency and enable light microscopy analysis of genetically-labelled fluorescent cells in whole organs, notably the brain[10,11,25,26] and subsequently in other organs[12,27]. However, while immunostaining has been achieved in embryos[28,29] and nerve tissue[10,11,28,30,31], analysis of other adult tissues has largely remained restricted to genetically encoded fluorescent proteins and broad-specificity stains including nuclear dyes and motif-detecting lectins[12,27,32]. In particular, immunolabelling of dense epithelial tissues and highly pigmented organs has remained an insuperable hurdle. FLASH addresses these problems by removing molecular barriers to allow free label diffusion into the tissue, increasing antigenicity and providing tissue-specific procedures for optimal clearing.

Development of FLASH

We initially developed FLASH for the epitope recovery in normal and transformed epithelia of the pancreas, liver and lung[1] after we had failed to immunolabel epithelial cells with previously published 3D-imaging techniques. The majority of whole-organ clearing protocols has been developed for brain and nervous tissue[10,11,15-17,26], which differs from other inner organs from the microanatomical to the biochemical level. Abdominal organs are hardly accessible by staining reagents due to the presence of serous membranes on the surface, epithelial barriers inside the organ, as well as

encapsulated organ compartments and abundant extracellular matrix. Whilst the brain has one of the highest water and fat contents, and is easily permeabilized by detergent washes, other inner organs are rich in proteins, which hinders permeabilization[33,34]. Furthermore, high concentrations of proteases and other enzymes may interfere with immunostainings if these tissues are insufficiently fixed. Thus, in contrast to the brain, inner organs require further treatment to restore antigenicity after tissue fixation, in addition to successful tissue clarification. We devised a succinct sequence of chemical treatments to unmask antigens in all cell compartments, distribute high molecular weight labels uniformly throughout the tissue, and achieve optical transparency whilst maintaining organ shape and tissue integrity (Fig. 1). Standard histology employs enzymatic digestion and pressure-cooking to retrieve antigens and enable immunostaining of paraffin-embedded tissue sections[35]. However, both proteolysis and heat have a detrimental effect on tissue architecture of native biological samples[36,37]. We hypothesised that a combination of tissue permeabilization and partial reversal of protein crosslinking would recover antigenicity without compromising tissue integrity. We assayed a range of different buffer systems, that are used in conventional histological tissue processing[38], in combination with detergent-mediated membrane solubilization and low heat, followed by antibody incubation in a solvent-rich blocking reagent[1]. Mild heat was necessary to achieve staining, but higher temperatures perturbed tissue integrity and caused sample loss (Extended Data Fig. 1a). Whilst previous tissue-clearing techniques alter tissue biochemistry to reduce light scatter and enhance organ transparency[10-12,25-27], FLASH specifically recovers masked epitopes and increases sample permeability to clear access for high molecular weight labelling agents such as antibodies and lectins[1] (Extended Data Fig. 1b).

Our original approach makes use of a sodium dodecyl sulphate (SDS)-based reagent (FLASH Reagent1) for antigen retrieval[1]. To further expand the range of FLASH compatible epitopes to proteins that may be disrupted by SDS, we evaluated alternative detergents to substitute for SDS in the sample antigen retrieval steps. Whilst we did not find satisfying results with non-ionic detergents, we observed that zwitterionic detergents efficiently recover pancreatic epitopes (Extended Data Fig. 1c). Zwittergent® 3-10 (hereafter referred to as Zwittergent) in combination with urea (FLASH Reagent2) produced robust immunostaining on all tissues analysed and improved the performance of difficult antibodies such as those recognizing

subcellular structures and nuclear proteins. FLASH Reagent2 improved imaging of the tubulin cytoskeleton and microsomes of liver cells (Extended Data Fig. 2a, b), and prevented damage of vulnerable samples such as embryos in comparison to Reagent1 (Extended Data Fig. 2c). Other subcellular structures such as the cilia of bronchiolar cells were well preserved both with Reagent1 and Reagent2 (Extended Data Fig. 2d). We hypothesise that the higher Critical Micelle Concentration (CMC) of Zwittergent (Supplementary Table 1) in combination with urea[39-41] aids the antigen retrieval of densely packed organs such as liver, but is not necessary for organs with a lower cellular density like lungs. Therefore, either FLASH Reagent1 or Reagent2 will be preferred depending on the tissue and antigens of interest (Supplementary Tables 2 and 3). After labelling, samples are immersed in a refractive index (RI) matching medium making use of the range of recently developed aqueous clearing solutions[5,10-12,27,32,42,43] and organic solvents[5,25,28,31,44] (Extended Data Fig. 3), achieving total tissue transparency (Fig. 2a). We have successfully applied FLASH to pancreas[1], brain, lung[1], liver[1], stomach, mammary gland and lacrimal gland, producing fluorescence distribution in three dimensions that are highly coherent with presentation in 2D tissue stainings (Fig. 2, 3, 4). The wide range of supported antibodies enables the simultaneous visualization of all tissue types, including ductal epithelia, stroma, nerves, muscles, vasculature and the lymphatic system as well as tissue-specific cell types such as hepatocytes, pancreatic acinar and lung alveolar cells (Fig. 2c, d; Figs. 3, 4; Supplementary Videos 1-6).

To further test the effect of FLASH processing on tissue morphology, we embedded FLASH Reagent2-treated organs in paraffin and analysed specimens previously imaged in three dimensions by conventional 2D histology. Despite the previous FLASH treatments and analysis, the tissue remained receptive to conventional histological evaluation by haematoxylin and eosin staining (Fig. 2d-f). Tissue architecture remained intact and different compartments such as blood vessels and ducts could readily be identified as in control tissue processed by conventional paraffin embedding (Fig. 2d-f). Thus, FLASH enables deep tissue immunolabelling of intact organs while maintaining tissue architecture and epithelial integrity.

Applications of FLASH

FLASH enables the three-dimensional (3D) molecular analysis of intact organs and tissue biopsies at subcellular resolution. A sequence of chemical tissue alterations

renders the samples susceptible for immunological labelling and histological staining whilst preserving cell and tissue integrity. We originally developed FLASH for quantifying cell types and morphological deregulations in intact adult organs such as the pancreas, lungs and liver of healthy and cancer-bearing mice[1]. More recently, we have introduced an adaptation of FLASH with a modified chemical composition to detect changes in the molecular organisation of the intercellular bridge at the end of cell division in mouse embryos[2]. To our knowledge, this is the first time these structures have been visualized within intact tissues. We have also used FLASH on fixed human biopsies (Fig. 4d), as well as heme-rich and highly pigmented whole organs such as the heart (Fig. 5a-d), the spleen (Fig. 5e-f) and organisms (*Drosophila melanogaster*; Fig. 5g). An adaptation for organoid clearing allows immunostaining of nuclear markers in expected foci (Figs. 6a, b), while preserving the integrity of subcellular structures such as midbodies (Fig. 6c). We use FLASH for studying epithelial malignancies such as pancreatic cancer (Fig. 7a, b), mammary gland cancer (Fig. 7c) and lung metastases (Fig. 7d, e). FLASH can also be used for imaging whole E13.5 mouse embryos (Fig. 8a; Supplementary Video 7) and E18.5 embryonic organs (Fig. 8b). FLASH-imaged tissues and organisms remain intact and can be subsequently analysed by conventional 2D histological analysis, which fully integrates FLASH into standard histopathology[45] (Fig. 2d). Altogether, FLASH is a versatile technique that can be used for answering a wide variety of questions throughout the biological sciences.

Overview of the Procedure

The main stages of the protocol are sample procurement (steps 1-25), permeabilization and epitope recovery (steps 26-29), staining (steps 30-38) and tissue clearing (steps 39-43; Fig. 1). FLASH has no specific requirements for tissue fixation and whilst a different fixative may be of advantage for certain antibody combinations, overnight fixation in 4% (wt/vol) paraformaldehyde (PFA) or 10% (vol/vol) neutral buffered formalin (NBF) achieved excellent results in our experiments. Where possible, an additional step for the removal of blood by cardiac perfusion with PBS can be included before sample fixation (step 11), or tissues can be depigmented to increase transparency (step 25). Similar to immunological stainings on tissue sections, unstained samples and isotype controls help the evaluation and interpretation of FLASH stainings (see Supplementary Methods –

'Guide for staining evaluation'). FLASH-treated samples are preferably analysed by optical-sectioning light microscopy to allow for spatial quantifications. Depending on the desired resolution and the sample volume to be captured, confocal, spinning disk, multi-photon or light-sheet microscopy may be preferable (step 64) (see Supplementary Methods – 'Microscopy Guide').

Limitations

FLASH is devised to study samples commonly analysed by histopathological workflows. It does not preserve life functions since samples are conventionally chemically fixed and need to be permeabilized to allow antibody penetration into deep tissue layers and cells. Consequently, FLASH, like all whole-organ clearing protocols, is limited to ex-vivo analysis. Highly pigmented tissues, such as samples with a high haem content can be difficult to clear[46] and we perform cardiac perfusion (Step 11) or additional depigmentation (step 25) to increase sample transparency. The utilization of FLASH for plant material has not yet been evaluated.

FLASH allows the detection of specific antigens as well as supportive tissues in the 3D context of unperturbed organ architecture from single-cell level to whole murine organs or human biopsies of lower or equivalent size (approximately 2 cm^3). Bigger samples may require longer incubation times and the maximum sample size is dependent on the microscope system (consult Supplementary Methods – Microscopy guide and Supplementary Table 3).

The researcher can use standard commercially available antibodies and, unlike other whole-organ clearing protocols[12,27], does not rely on prior genetic labelling. Antibody performance is similar to stainings on tissue sections (Fig. 2b; 3c, d; 4a, c), which we recommend to include as controls when a new antibody is tested. Antibodies with low sensitivity in 2D sections are unlikely to improve in 3D stainings.

Even after antigen retrieval, antibody penetration in very dense tissues such as tumours require longer incubation times (Supplementary Table 3). Smaller Fragment antigen-binding (Fab) and single-domain antibodies (nanobodies) penetrate more efficiently and hold potential to further reduce incubation times for immunostaining[47,48] (Extended Data Fig. 4). While the commercial availability of Fabs and nanobodies is still limited, these expanding technologies are improving the efficiency of 3D immunolabelling protocols[49,50].

.

Comparison with other approaches

Optical clearing of entire organs has been performed for over 100 years and many excellent recent approaches tailored clearing protocols to detect genetically encoded fluorescent markers in the brain[12] and later whole body of an adult mouse[27], or detect and map the spatial relationships of neuronal cell types[11,17,24,26]. Optical clearance is commonly achieved in a multi-step treatment comprising depigmentation, membrane solubilisation, lipid removal and RI-matching. Most alternative approaches have been tailored to fragile nervous tissues and use extensive crosslinking and long washes at mild temperature to remove lipids without perturbing the intricacy of neuronal circuitry[30,50,51]. A range of detergents have been used for membrane solubilisation: iDISCO[28] (Na-deoxycholate, NP40, TritonX-100, Tween-20), CLARITY/SWITCH[11,30] (SDS), CUBIC[12] (Quadrol, TritonX-100), AbScale[51] (TritonX-100). In our development of FLASH, we tested a range of buffers and detergents, and found that SDS, previously used in CLARITY, produces robust optical clearing after short incubation times. In contrast to CLARITY, FLASH Reagent1 requires a narrow incubation temperature range around 54°C to achieve clearance and enable immunolabeling (Extended Data Fig. 1). As an advantage, FLASH does not benefit from extensive sample crosslinking to a hydrogel matrix, previously used for reconstructing neuronal networks[36] and expansion microscopy[52,53], and is consequently less toxic and faster as it does not depend on extended incubations or active electrophoresis to achieve transparency. Furthermore, the chemical treatments in previous approaches require strict formulations of RI-matching media. In contrast, we found that FLASH treated samples are compatible with a range of both aqueous or dehydrating mediums which allows to tailor FLASH-based analyses to the experimental and microscope requirements (Extended Data Fig. 3).

FLASH Reagent2 utilises high concentrations of urea, similar to AbScale and CUBIC, but critically depends on the inclusion of a zwitterionic detergent to achieve antigen retrieval. Indeed, we first discovered Zwittergent in a urea-free detergent screen (Extended Data Fig. 1c) and added urea later as we found it to improve homogeneous staining in highly compartmentalized tissues. Zwittergent provides tissue permeability and easier removal of residual detergent due to its higher critical micelle concentration (CMC) compared to ionic detergents[39]. In addition, it is less

denaturing and protects the native state of proteins due to the lack of net charge on the hydrophilic head groups[54]. In combination with urea, which breaks hydrogen bonds[41], Zwittergent offers a balance between permeabilization and preservation of epitope and tissue integrity.

We performed a comparison of FLASH with recent techniques for tissue permeabilization and clearing, AbScale[51], SWITCH[30], CUBIC HistoVIsion[50] and iDISCO[28]. Among these techniques, FLASH is the fastest (Extended Data Fig. 5a). In our hands, transparency of 500 µm brain slices was achieved in all techniques, but pancreata only cleared with FLASH, CUBIC HistoVIsion and iDISCO, and mammary glands only with FLASH and iDISCO (Extended Data Fig. 5b). We compared immunolabelling using a range of well-established antibodies that give excellent results in 2D immunofluorescence. Whilst antibodies readily detected neurons, astroglia and vessels in the brain (even in untreated samples; Extended Data Fig. 6), the same antibodies failed to find their epitope in the pancreas except for FLASH-treated samples (Extended Data Fig. 7a). Epithelial markers, like c-peptide, could be detected only partially in CUBIC and iDISCO (Extended Data Fig. 7b). Others, like keratin-19, a robust duct cell marker, could only be detected with FLASH (Extended Data Fig. 7). Antigens of the mammary gland were labelled specifically and throughout the tissue depth only with FLASH and iDISCO (Extended Data Figs. 8 and 9). In conclusion, when selecting a 3D imaging technique, the tissue and epitopes of interest should be considered (Supplementary Table 4). We present FLASH as the optimal technique for immunolabelling of dense inner organs.

Materials

Biological materials:

- Animal samples. Our laboratory works with mice of FvB background for mammary gland tumour models and C57BL6/J or mixed backgrounds for other purposes (there are no requirements for specific strains). Experiments or tissue labelling on living animals such as dextran intravenous injection as described in steps 1-5 of the Procedure can be performed before humane culling. ! CAUTION animal maintenance, husbandry and experiments must be performed following national and institutional legislation. All our animal experiments have been approved by the London Research Institute Animal

Ethics Committee or the Animal Welfare and Ethical Review Body of the Francis Crick Institute and conform to UK Home Office regulations under the Animals (Scientific Procedures) Act 1986 including Amendment Regulations 2012.

- Clinical (human) samples. Human resections can be fixed as per standard hospital practice before analysis by FLASH[45]. We recommend removing traces of surgical ink which can interfere with light microscopy, and to depigment samples. ! CAUTION all experiments must be performed in accordance with relevant guidelines and regulations regarding informed consent from patients. Our use of human tissue samples was approved by the NHS Health Research Authority following assessment by a Research Ethics Committee (HSC REC B; reference 16/NI/0119).

Reagents:

! CAUTION All safety and hazard indications listed below were consulted in https://pubchem.ncbi.nlm.nih.gov

Vasculature labelling:

- Fluorescein isothiocyanate-dextran (Dextran-FITC; Sigma-Aldrich, cat. no. FD2000S)
- DyLight 594 labeled Lycopersicon esculentum Lectin (Lectin-594; Vector Laboratories, cat. no. DL11771)

  CRITICAL Work under a sterile laminar flow cabinet when diluting dyes for intravenous injection.
- Ethanol absolute (EtOH; Sigma-Aldrich, cat. no. 24105)

  ! CAUTION EtOH is highly flammable (liquid and vapour), avoid contact with ignition sources and incompatible materials such as oxidisers, and store appropriately as indicated by the provider.

FLASH:

- DPBS, no calcium, no magnesium (PBS; Thermo Fisher Scientific, cat. no. 14190094)

- Formalin solution, neutral buffered, 10% (vol/vol) (NBF; Merck, cat. no. HT501128)
- Affymetrix Paraformaldehyde Solution, 4% (wt/vol) in PBS (PFA; Fisher Scientific, cat. no. 199431LT)

  ! CAUTION Formaldehyde derivatives are toxic if swallowed, inhaled or in contact with the skin. They cause severe skin burns and eye damage. They may cause cancer. Handle with care and appropriate PPE (gloves, mask, lab coat and protective goggles) and under a fume hood.
- Hydrogen peroxide 60% (wt/vol) (200 volumes), Extra Pure SLR, Fisher Chemical (H_2O_2; Fisher Scientific, cat. no. H/1862/15)

  ! CAUTION H_2O_2 is a strong oxidizer and may cause fire or explosion. It is harmful if swallowed or inhaled, and can cause severe skin and eye damage. Handle with care and appropriate PPE (gloves, mask, lab coat and protective goggles) and under a fume hood. Avoid contact with flammable substances.
- Dimethyl sulfoxide (DMSO; Sigma-Aldrich, cat. no. D2650)

  ! CAUTION DMSO causes skin and severe eye irritation. May cause respiratory tract irritation. Handle with care and appropriate PPE (gloves, mask, lab coat and protective goggles) and under a fume hood.
- Agarose, low gelling temperature (Sigma-Aldrich, cat. no. A9414)
- Superglue
- Sodium dodecyl sulphate (SDS) ³ 98.0%, specially pure (SDS; VWR, cat. no. 442444H)

  ! CAUTION SDS is harmful if swallowed, and causes serious skin, respiratory tract and eye irritation. Handle with care and appropriate PPE (gloves, mask, lab coat and protective goggles) and under a fume hood.
- ZWITTERGENT® 3-10 Detergent – CAS 15163-7 – Calbiochem (Zwittergent; Merck, cat. no. 693021)

  ! CAUTION Zwittergent causes serious skin, respiratory tract and eye irritation. Handle with care and appropriate PPE (gloves, mask, lab coat and protective goggles) and under a fume hood.
- Urea (Sigma-Aldrich, cat. no. U5378)
- Boric acid (Sigma-Aldrich, cat. no. B6768)

! CAUTION Boric acid may damage fertility or the unborn child. Handle with care and appropriate PPE (gloves, mask, lab coat and protective goggles) and under a fume hood.

- Triton™ X-100 (Merck, cat. no. T9284)

  ! CAUTION Triton™ X-100 is harmful if swallowed, and causes serious skin, respiratory tract and eye irritation. Handle with care and appropriate PPE (gloves, mask, lab coat and protective goggles) and under a fume hood.
- Sodium azide (Sigma-Aldrich, cat. no. S8032)

  ! CAUTION Sodium azide is fatal if swallowed. Handle with care and appropriate PPE (gloves, mask, lab coat and protective goggles) and under a fume hood.
- Gibco™ Fetal Bovine Serum, qualified, heat inactivated, E.U.-approved, South America Origin (FBS; Fisher Scientific, 10500064)
- Bovine Serum Albumin (BSA; Sigma-Aldrich, cat. no. A7906)
- Primary antibodies (see table 1)
- Secondary antibodies (see table 1)
- Lectins (see table 1)
- eBioscience™ DRAQ5™ (DRAQ5; Thermo Fisher Scientific, cat. no. 65-0880-92)
- DAPI (Merck, cat. no. 10236276001)
- Methanol (MetOH, Merck, cat. no. 32213-M)

  ! CAUTION MetOH is highly flammable (liquid and vapour). It is toxic if swallowed, inhaled or in contact with the skin. It causes damage to organs. Handle with care and appropriate PPE (gloves, mask, lab coat and protective goggles) and under a fume hood.
- Methyl salicylate (MetSal; Merck, cat. no. M6752)

  ! CAUTION MetSal is harmful if swallowed. It can cause skin and eye irritation. Handle with care and appropriate PPE (gloves, mask, lab coat and protective goggles).
- Benzyl Alcohol (BA; Merck, cat. no. 108006)

  ! CAUTION BA is harmful if swallowed or inhaled. Handle with care and appropriate PPE (gloves, mask, lab coat and protective goggles) and under a fume hood.

- Benzyl Benzoate (BB; Merck, cat. no. B6630)

  ! CAUTION BB is harmful if swallowed. Handle with care and appropriate PPE (gloves, mask, lab coat and protective goggles).

Table 1 | Antibodies*

Primaries (antigens)	Abbreviation	Dilution	Raised in	Catalogue no	RRID
a-smooth muscle actin	SMA	1:100	Mouse	Sigma-Aldrich A5228	AB_262054
a1 Na/K ATPase	ATPase	1:100	Mouse	Abcam ab7671	AB_306023
Acetylated tubulin	Ac-tubulin	1:100	Mouse	Sigma-Aldrich T7451	AB_609894
Amylase	Amy	1:50	Goat	Santa Cruz sc-12821	AB_633871
Aquaporin 1	Aqp1	1:100	Rabbit	Sigma-Aldrich HPA019206	AB_1844965
Aurora B	AurB	1:100	Mouse	BD 611082	AB_2227708
Cadherin 1	Cdh1	1:100	Rat	Thermo Fisher 13-1900	AB_2533005
CD16	CD16	1:100	Mouse	Thermo Fisher MA1-7633	AB_2103889
CD3	CD3	1:100	Rabbit	Abcam ab5690	AB_305055
CD31	CD31	1:100	Rabbit	Abcam ab28364	AB_726362
CD44	CD44	1:100	Rat	Merck MAB2137	AB_2076454
CD45R	B220	1:100	Rat	Biolegend 103202	AB_312987
Clara Cell secretory protein	CC10	1:100	Goat	Santa Cruz sc-9772	AB_2238819
Cleaved caspase 3	CC3	1:100	Rabbit	R&D AF835	AB_2243952
Collagen IV	ColIV	1:50	Goat	Sigma-Aldrich AB769	AB_306025
Connecting peptide	C-pep	1:100	Rabbit	CST 4593	AB_10691857
Cytochrome P450	Cyt P450	1:100	Mouse	Abcam ab22717	AB_447282
Cytokeratin 19	Krt19	1:100	Rat	DSHB TROMA-III	AB_2133570
Cytokeratin 5	Krt5	1:100	Mouse	Biotechne NBP2-22194	AB_2857967
Cytokeratin 8	Krt8	1:100	Rat	DSHB TROMA-I	AB_531826
Forkhead box protein P1	FoxP1	1:100	Rabbit	CST 2005	AB_2106979
Gastric Intrinsic Factor	GIF	1:100	Rabbit	Sigma-Aldrich HPA040774	AB_10795626
Glial Fibrillary Acidic Protein	GFAP	1:100	Rabbit	Abcam ab7260	AB_305808
Glutamine synthetase	GS	1:100	Rabbit	Abcam ab73593	AB_2247588
Green Fluorescent Protein	GFP	1:100	Goat	Abcam ab6673	AB_305643
Keratin 14	Krt14	1:100	Mouse	Abcam ab9220	AB_307087
Mist1	Mist1	1:100	Mouse	Santa Cruz sc-80984	AB_2065216
Mucin-1	Muc1	1:100	Rabbit	Abcam ab15481	AB_301891
Mucin-5AC	Muc5AC	1:100	Goat	Santa Cruz sc-16903	AB_649616
Neuroendocrine convertase 1	PCSK1	1:100	Rabbit	Millipore SAB1100416	AB_10606261
Podoplanin	Pdpn	1:50	Goat	R&D AF3244	AB_2268062
Proliferating cell nuclear antigen	PCNA	1:100	Rabbit	Santa Cruz sc-7907	AB_2160375

Proliferation marker Ki67	Ki67	1:100	Rabbit	Abcam ab16667	AB_302459
Prospero homeobox protein 1	Prox1	1:100	Rabbit	Abcam ab101851	AB_10712211
Red Fluorescent Protein	RFP	1:100	Rabbit	Rockland 600-401-379	AB_2209751
S100	S100	1:100	Rabbit	Dako Z0311	AB_10013383
Surfactant Protein C	SFTPC	1:100	Rabbit	Sigma-Aldrich HPA010928	AB_1857425
Tubulin	Tub	1:50	Rat	Abcam ab6161	AB_305329
Tyrosine hydroxylase	TH	1:100	Rabbit	Merck AB152	AB_390204
Vimentin	Vim	1:100	Chicken	Sigma-Aldrich AB5733	AB_11212377
Wilms Tumour 1	WT1	1:100	Rabbit	Santa Cruz sc-192	AB_632611
Lectins	**Abbreviation**	**Dilution**	**Raised in**	**Catalogue no**	**RRID**
DBA-FITC (lectin)	-	-	-	Vector labs FL-1031	AB_2336394
DBA-Rhodamine (lectin)	-	-	-	Vector labs RL-1032	AB_2336396
PNA-FITC (lectin)	-	-	-	Vector labs FL-1071	AB_2315097
Conjugated antibodies	**Fluorophore**	**Dilution**	**Raised in**	**Catalog no**	**RRID**
Anti-Chicken IgY	FITC	1:250	Donkey	Thermo Fisher SA1-72000	AB_923386
Anti-goat IgG	AF 546	1:100 - 1:1000	Donkey	Thermo Fisher A-11056	AB_2534103
Anti-goat IgG	AF 647	1:100 - 1:1000	Donkey	Thermo Fisher A-21447	AB_2535864
Anti-mouse IgG	AF 488	1:100 - 1:1000	Donkey	Thermo Fisher A-11055	AB_2534102
Anti-mouse IgG	AF 546	1:100 - 1:1000	Donkey	Thermo Fisher A-10036	AB_2534012
Anti-mouse IgG	AF 594	1:100 - 1:1000	Donkey	Thermo Fisher A-21203	AB_2535789
Anti-mouse IgG	AF 700	1:100 - 1:1000	Goat	Thermo Fisher A-21036	AB_2535707
Anti-rabbit IgG	AF 546	1:100 - 1:1000	Donkey	Thermo Fisher A-10040	AB_2534016
Anti-rabbit IgG	AF 647	1:100 - 1:1000	Donkey	Thermo Fisher A-31573	AB_2536183
Anti-rat IgG	AF 488	1:100 - 1:1000	Donkey	Thermo Fisher A-21208	AB_2535794
Anti-rat IgG	AF 594	1:100 - 1:1000	Donkey	Thermo Fisher A-21209	AB_2535795
Anti-rat IgG	AF 647	1:100 - 1:1000	Donkey	Abcam 150155	AB_2813835
GFP sdAb - FluoTag-Q	ATTO 488	1:100	Alpaca	SYSY N0301-At488-S	AB_2744617

*An extended version of this table is available (Supplementary Table 2).

Equipment:

Consumables:

- Steriflip-GP Sterile Centrifuge Tube Top Filter Unit (sterile filter tube; Merck, cat. no. SCGP00525)
- BD Medical™ BD Micro-Fine™ Insulin Syringe (Fisher Scientific, cat. no. 16131931)
- Dispocut Board White – A5 (148x210mm) (dissection boards, CellPath, cat. no. CGB-0502-53A)

- Dissection tools (Fine Science Tools)
- BD Plastipak 20 mL sterile disposable graduated eccentric luer slip syringe (BD Plastipak, cat. no. 300613)
- Terumo™ Agani™ Single-use Sterile Hypodermic Needles (Fisher Scientific, cat. no. 15428652)
- Corning® 50 mL PP centrifuge tubes, self-standing (Merck, cat. no. CLS430921)
- Peel-A-Way™ embedding molds (Merck, cat. no. E6032)
- Derby Extra Double Edge Safety Razor Blades (for vibratome)
- Wheaton® 224884 Lab File™ Clear Glass Sample Vials for Aqueous Samples with 15-425 Size Phenolic Rubber-Lined Screw Caps (Wheaton vials; Capitol Scientific, cat. no. 224884)
- 1000 µL Graduated Tip (Star Lab, cat. no. S1111-6700)
- 200 µL Tip (Star Lab, cat. no. S1111-0700)
- 10/20 µL XL Graduated Tip (Star Lab, cat. no. S1110-3800)
- Aluminium foil
- Embedding cassettes, Simport Scientific (VWR, cat. no. 60872-510)
- Lids for Embedding Cassettes, Simport Scientific (VWR, cat. no. 87002-382)
- Fisherbrand™ Foam Biopsy Pads, Rectangular foam pad (Fisher Scientific, cat. no. 22-038-223)
- Argos Technologies Transfer Pipette, 7.5 mL, General Purpose (Cole-Parmer, cat. no. UY-06226-11)
- Circular coverglasses 24 mm diameter (Agar Scientific, cat. no. L46R24)
- Rectangular coverglasses 35 x 64 mm (Agar Scientific, cat. no. L463564)
- m-Slide 8 Well Glass Bottom (IBIDI, cat. no. 80827)
- 1.5 mL SuperLock Microcentrifuge Tube, Natural (Star Lab, cat. no. 11415-5100)

Bench apparatus

- Small Animal Recovery Chamber (hot box, Vet Tech solutions)
- Mouse restrainer for intravenous injections (Vet Tech solutions)
- IncuSafe Multigas Incubator (PHCbi, cat. no. MCO-170MUVH-PE)
- Class II Microbiological Safety Cabinet Envair Eco Safe Comfort (Wolflabs, cat. no. O00002120010)

- Fisherbrand™ Nutating Mixers – Variable Speed (Fisher Scientific, cat. no. 88-861-044)
- Microwave oven
- Leica VT1200 S Fully automated vibrating blade microtome (Vibratome; Leica Biosystems, cat. no. 1491200S001)

  ! CAUTION Cut hazard. Handle the vibratome with care.
- HB-1D hybridiser (Techne, cat. no. FHB1DQ)
- Magnetic Stirrer with Heating (Star Lab, cat. no. N2400-3010)
- Scienceware F371220040 Polygon Spinbar, Magnetic Stir Bar w/Ring, 40 x 8 mm (Cole-Parmer, cat. no. UY-04775-13)
- Pyrex Squat Beaker – 250 ml (Breckland Scientific, cat. no. BEG-200-250)
- Pyrex Squat Beaker – 25 ml (Breckland Scientific, cat. no. BEG-200-025)
- Pyrex Vista 70024-5 Graduated Glass Cylinder, 25 mL (Cole-Parmer, cat. no. UY-34504-71)
- Milli-Q® Advantage A10 Water Purification System (Merck, cat. no. Z00Q0V0WW)
- Watch Glass, Square, 1 5/8 inches (Carolina®, cat. no. 742300)
- Tubular extraction arm Movex ME Type 1500-75 (Movex, cat. no. MET 1500-75)

Microscopes:

- Stereomicroscope. For tissue microdissection we use Zeiss Stemi SV11 Stereomicroscope (Zeiss).
- Upright Light-sheet fluorescent microscope (LSFM) with macrozoom. For whole-organ imaging, we use the Miltenyi-LaVision Biotech UltraMicroscope II equipped with the following laser lines: 488nm, 561nm, 638nm, 705nm and 785nm. For signal detection an Olympus MVPLAPO 2X NA 0.5 objective lens, protective dipping cap (WD > 5.7 mm) and Andor ZYLA-5.5-CL10 camera were used.
- Confocal microscope. For studies that require subcellular resolution, we use an inverted Zeiss LSM 780 confocal microscope (Zeiss) equipped with a 405 nm laser, an argon laser, a DPSS 561 nm laser, a HeNe 594 nm laser and a HeNe 633 nm laser using the following objective lenses: 10x/0.45 Ph2 Plan-

Apochromat, 25x/0.8 LD LCI Plan Apochromat and 40x/1.4 Oil DIC M27 Plan-Apochromat.

Computer and software

- Image analysis and processing is performed using a dedicated imaging workstation with the following characteristics: SSD: 960 EVO 1TB; HDD: ATA TOSHIBA DT01ACA2 SCSI; RAM: 128 GB; processors: Intel® Xeon® CPU E5-2667 v4 @3.20GHz (2 processors); OS: Windows 10 Enterprise; GPU: NVIDIA GeForce GTX 1080 Ti; network connection: 10GB/s link.
- Fiji[55] for general image analysis, (tiling and 3D rendering).
  https://imagej.net/Fiji
- BigStitcher[56] (Fiji plugin) for manual tile stitching (recommended).
  https://imagej.net/BigStitcher
- LaVision BioTec Imspector Pro (TeraStitcher plugin[57]) for automatic tiles stitching.
  https://www.lavision.de/en/downloads/software/
- Imaris x64 9.5.1 (Bitplane – Oxford Instruments) is used for 3D rendering, gamma correction, visualisation, morphometric quantifications and for recording images and movies for publication.
  https://imaris.oxinst.com

Reagent setup:

Depigmentation solution

Dilute DMSO and H_2O_2 in PBS in 1:1:4 (vol:vol:vol) ratio. Depigmentation solution should be prepared fresh before every use.

Borate

Prepare a working solution of borate 200 mM (12.36 g/L) by dissolving boric acid in milli-Q H_2O with a magnetic stirrer. Adjust the pH to 7.0 with NaOH. Borate may be stored at room temperature (RT, 21°C) indefinitely.

FLASH Reagent1

For SDS-based antigen retrieval, add 4% (wt/vol) SDS (40 g/L) to 200 mM borate. SDS-based antigen retrieval solution may be stored at RT indefinitely.

FLASH Reagent2

For Zwittergent-urea-based antigen retrieval, dissolve urea in borate to a concentration of 250 g/L. CRITICAL Urea dissolution is an endothermic reaction. Zwittergent does not dissolve properly in the resulting cold solution. Incubate the urea-boric acid solution in a water bath or similar below 37°C until it reaches RT. Dissolve Zwittergent (80 g/L) in the warmed urea-borate solution. Zwittergent-urea-based antigen retrieval solution can be stored at 4°C for up to 8 weeks. Zwittergent precipitates at 4°C. Before using Zwittergent-urea-based antigen retrieval solution stored at 4°C, bring to RT rocking in a nutator until complete re-dissolution.

PBT

Prepare a solution of 0.2% (vol/vol) Triton™-X100 in PBS in a magnetic stirrer. PBT may be stored at RT indefinitely.

Blocking buffer

Prepare a solution of FBS 10% (wt/vol), sodium azide 0.02% (wt/vol), BSA 1% (wt/vol) and DMSO 5% (vol/vol) in PBT. Filter using a 20mm sterile filter to purify from undissolved BSA aggregates. Blocking buffer may be stored at 4°C for up to 4 months.

CRITICAL Other immunofluorescence protocols recommend blocking in serum of the species in which the secondary antibody was raised. In our hands, FBS and BSA work well for all donkey and goat-raised secondary antibodies utilised (see Table 1 and Supplementary Table 1).

DAPI

For nuclear staining of organoids, prepare a stock solution of 2 mg/mL in Milli-Q H_2O. Use 1:1000 (vol:vol) (final concentration of 2 mg/mL). DAPI stock solution may be stored frozen at -20°C protected from light indefinitely.

BABB

Mix BA and BB at 1:2 (vol/vol) and store at RT protected from light indefinitely.

Equipment setup:

Vibratome settings

Set the vibratome to 0.80 mm/s speed, 1 mm amplitude and 500 mm Auto Feed (slice thickness). Set to “Auto” (automatic) and “Cont” (continuous slicing).

Setup of LaVision Ultramicroscope II

Before starting the sample acquisition, light sheets alignment in MetSal (refractive index of 1.536) has to be performed using the LaVision calibration tool.

! CAUTION while MetSal fumes are not toxic, its odour is strong and may be unpleasant for some people. A tubular extraction arm (illustrated in Fig. 1) is recommended.

Setup of inverted Zeiss LSM 780

Seek expert guidance from your local imaging facility to set up the microscope. General guidelines for confocal microscopy can be consulted on this tutorial[58].

Procedure

! CAUTION All experiments in living animals must be performed following the appropriate legislation.

CRITICAL The procedure below is tailored for clearing and staining mouse tissues, embryos or human biopsies. When using insects, proceed directly to Step 12. For collecting and imaging organoids, see Box 1.

(Optional) Mouse vasculature labelling. Timing 30 min

CRITICAL Perform this labelling for imaging vasculature of any mouse organ. Alternatively, immunostain endothelium or other vascular cells (Table 1).

1. Pre-warm the hot box to 38°C for 5 min.
2. Place the mouse inside the hot box for 5-8 min. ! CRITICAL STEP Do not exceed 8 min as this could lead to dehydration of the mouse.
3. Place the mouse in the mouse restrainer for intravenous injection.
4. Gently wipe the tail with ethanol to disinfect and improve visibility of tail veins.

5. Inject 100 µL of 12 mg/mL FITC-conjugated Dextran or Lectin-594 using a 50U insulin syringe on the tail vein. Proceed to the next step 30 sec after injection.

Euthanasia, dissection, perfusion and fixation. Timing 1d

6. Euthanize mice by a method in line with the national regulations of animal welfare. In our lab we use cervical dislocation.
7. Pin the mouse to a dissection board in supine position.
8. Wipe the skin with 70% (vol/vol) ethanol.
9. Perform a midline laparotomy, avoiding damage to the organs of interest. Sterile conditions are not essential.
10. Cardiac perfusion: for lung collection, make a small incision in the left atrium and perfuse with 20 mL of PBS through the right ventricle. For collection of other organs, make a small incision in the right atrium and perfuse with 20 mL of PBS through the left ventricle.

    CRITICAL STEP If collection of both lungs and other organs is necessary, perform the perfusion through the left ventricle.

    CRITICAL STEP For detection of low expressed proteins, perform an additional perfusion with 20 mL of PFA 4% (wt/vol).
11. Dissect the mouse with surgical tools, avoiding any damage to tissues. The same tools may be used throughout the dissection. If dissecting the brain turn the mouse into prone position.
12. Fix the samples overnight at RT in 50 mL of 10% (vol/vol) NBF or 4% (wt/vol) PFA. If working with insects, rinse briefly in 100% EtOH to dissolve the hydrophobic lipid layer from the cuticle, then rinse in PBS before fixing in 4% (wt/vol) PFA and proceed to step 23.

    CRITICAL STEP Keep the organs in fixative in the conditions specified above. Under- and over-fixation can reduce the antibody labelling efficiency.

Tissue preparation and antigen retrieval. Timing 1d.

13. Wash the organs 10 min in 50 mL PBS on a nutator at RT.
14. Under the stereomicroscope, remove any non-desired tissue such as fat, fibres or remains of contiguous organs.

    ? TROUBLESHOOTING

15. ***Optional: Vibratome slicing (Steps 15-22):*** If the goal is to image subcellular structures of large organs or the working distance of the available objectives does not allow to image into deeper tissue layers, the samples can be sliced on a vibratome. If slicing in the vibratome is not required, proceed to step 23. First, prepare 4% (wt/vol) low gelling temperature agarose in ddH_2O. Microwave and keep at RT for 3-4 min.

    ! CAUTION Burn hazard. Do not heat the agarose in a closed bottle. Handle the hot agarose with care.

    CRITICAL STEP Avoid placing the samples in hot agarose, as this may damage the tissue.

16. Embed the organs in 4% (wt/vol) agarose on embedding moulds.
17. Wait for agarose polymerisation. This step may be performed at 4°C to reduce the polymerisation time.
18. Set up the vibratome (see Equipment Setup).

    ! CAUTION Cut hazard. Handle the vibratome with care.

19. Fill the vibratome tissue chamber with PBS
20. Glue the agarose cube to the vibratome tissue platform. Wait until the superglue dries before immersing the platform in the chamber.
21. Start the automatic slicing program.
22. Gently remove the agarose from the tissue slices and proceed to the next step.
23. Optional: For highly pigmented tissue, such as spleen, heart, human biopsies (see a list of examples in Supplementary Table 3), incubate the tissue in 50 mL depigmentation solution rotating overnight at RT. Wash 3 times in 50 mL PBS rotating for 20 min at RT. For removing chitin pigments in insects, bleach in 5 mL 35% (vol/vol) H_2O_2 for 16 h and wash in PBS overnight[59].

    ! CAUTION In contact with tissues, hydrogen peroxide is catalysed to H_2O and O_2. Oxygen production increases the pressure inside sealed tubes and can damage them. Place the tissue in depigmentation solution on an open tube for several min before sealing and incubating overnight.

    PAUSE POINT The samples can be stored in PBS at 4°C for one week. Alternatively, tissues may be gradually dehydrated (50 mL each of 30%-50%-70%-2x 100% (vol/vol) MetOH in ddH_2O, 30 min per step) and stored at -80°C for several months. To proceed from frozen samples, gradually rehydrate (50

mL each of 90%-70%-50%-30% (vol/vol) MetOH in ddH_2O and 2x PBS, 30 min per step).

24. Place organs or tissue slices in 50 mL antigen retrieval solution.
    CRITICAL STEP use FLASH Reagent1 for clearing adult organs. Use the milder FLASH Reagent2 for vulnerable tissues such as whole embryos or embryo organs, or for down-stream imaging of subcellular structures. Consult Supplementary Tables 2 and 3 for selecting the ideal treatment.
25. Incubate for 1 h in a nutator at RT.
26. Incubate at 54°C, rotating gently in a Thermomixer (small samples) or hybridizing oven (whole adult organs) overnight.
    CRITICAL STEP Do not incubate organs in FLASH Reagent1 for more than 16 h as this may damage the tissue. Organs in FLASH Reagent2 can be incubated for 24 h.
    ? TROUBLESHOOTING

Blocking and immunolabelling. Timing 4 d.

27. Wash samples 3x for 1 h in 50 mL PBT in a nutator at RT.
28. Move samples to a Wheaton vial.
    ? TROUBLESHOOTING
29. Incubate in blocking buffer (usually 500-1000 µL, see recommended volumes per sample type in Supplementary Table 3) for at least 1 h on a nutator at RT.
    PAUSE POINT Samples can be stored in PBT for 3 days at 4°C.
30. Add the primary antibodies to the blocking buffer (see antibody-specific recommended dilutions in Table 1 and Supplementary Table 2).
31. Incubate for at least 2 nights on a nutator at RT (see incubation time recommendations per sample type in Supplementary Table 3).
32. Wash 3 x 20 min in 9 mL PBS on a nutator at RT.
33. Add the secondary antibodies, fluorescent lectins and/or nuclear dyes in blocking buffer (see antibody-specific recommended dilutions in Table 1 and Supplementary Table 2).
34. Incubate for at least 2 nights on a nutator at RT in the dark (see incubation time recommendations per sample type in Supplementary Table 3).

CRITICAL STEP Secondary antibodies, fluorescent lectins and nuclear dyes are light-sensitive. Perform the above incubation and the following steps covering the samples in aluminium foil.

PAUSE POINT Samples can be stored in the staining solution at 4°C for 3 days.

Dehydration and clearing. Timing 5 h.

CRITICAL We commonly clear all FLASH-treated samples in MetSal. However, FLASH is compatible with a range of aqueous or dehydrating RI-matching media. The final RI, as well as effects on sample size and imaging depth vary with each medium and should be taken into consideration (Extended Data Fig. 3). For high resolution imaging, the RI-medium should also be chosen to match with the available objective lenses. A dedicated section can be found in the microscopy guide in the supplementary information (Supplementary Methods). Steps 36-39 apply for clearing with MetSal or BABB. For alternative clearing strategies see Supplementary Methods.

35. Wash 3 x 20 min in 9 mL PBS on a nutator at RT.
36. (Optional) For imaging of whole organs or embryos under the LSFM, samples may be embedded in 1% (wt/vol) low gelling temperature agarose in ddH_2O (optional step). For agarose preparation, precautions, embedding and polymerisation, see steps 15-17. Perform the following steps on the entire agarose block.
37. Gradually dehydrate in 4-9 mL each of 30%-50%-75%-2x 100% (vol/vol) MetOH in H_2O, at least 30 min per step.

    CRITICAL STEP: For large whole organs or embryos, perform the dehydration in the Wheaton vials to preserve their shape.

    CRITICAL STEP: For tissue slices and relatively flat organs such as the mammary gland or pancreas, move to an embedding cassette sandwiched between thin biopsy pads. Dehydrate the entire cassette mount in a 250 mL beaker.

    CRITICAL STEP 30 min is the minimum length for dehydration steps. Shorter steps may not be sufficient for complete dehydration. Water traces emulsify in MetSal or BABB, considerably reducing organ clarification.
38. Transfer the samples to watch glasses in 100% MetOH.

39. Gradually clear in 4-9 mL each of 25%-50%-75 2x 100% (vol/vol) MetSal (or BABB) in MetOH, 30 min per step, or until samples have sunk to the bottom. Note clarification will become apparent after incubation in 50% (vol/vol) MetSal (or BABB).

    ! CAUTION Methyl salicylate dissolves polystyrene. Prepare dilutions in a 25 uL Pyrex beaker. BABB can be used with polypropylene tubes.

    ? TROUBLESHOOTING

    PAUSE POINT Samples may be stored immersed in 100% MetSal or BABB in the dark at RT for up to 2 weeks. Tissues in MetSal or BABB should be stored at RT at all times, as water condensation at 4°C or lower will emulsify and affect tissue transparency.

Box 1: Organoid workflow: Timing 2 d from collection to imaging.

CRITICAL The organoid workflow from collection to imaging differs significantly in terms of procedures and timing from the workflow for tissue. This alternative application of FLASH antigen retrieval is necessary for robust staining of certain antigens. FLASH is demonstrated in Fig. 6 using dense murine mammary tumour (MMTV-PyMT[60]) organoids.

Procedure:

1. Plate epithelial cells resuspended in Matrigel™ in a 25 μL dome in an 8-well chamber slide.
2. Allow the Matrigel™ to polymerise in a cell culture incubator at standard conditions (37°C, 5% CO_2, 20% O_2).
3. Add 250 μL of organoid media to cover the Matrigel™ dome.
4. Place in a cell culture incubator at standard conditions. Perform any required experiments (stimulation, treatment etc).

    CRITICAL STEP Organoids grow at different rates depending on the organ of origin, malignancy etc. MMTV-PyMT organoids established from single cells reach the maximum size 5-7 days after plating.
5. Aspirate media.
6. Wash Matrigel™ dome with 300 μL PBS.
7. Fix in 5% (vol/vol) NBF or 4% (wt/vol) PFA for 10 min.

8. Gently remove the fixative with a P200 pipette from the corner of the well.

    CRITICAL STEP Fixatives soften the Matrigel™ dome and many organoids can be lost from this step onwards. Pipetting carefully and with a P200 is necessary to minimise organoid loss.

9. Wash 3 x 300 µL PBS for 20-30 sec per step.
10. Apply 300 µL of FLASH Reagent2 for 2 h at RT, rocking gently on a nutator.
11. Wash 5 x 300 µL PBT for 10 min per step.
12. Block in 300 µL blocking solution for 30 min.
13. Prepare a 200 µL/well dilution of primary antibodies (Table 1 and Supplementary Table 2) in a 1.5 mL centrifuge tube (1:200 in blocking buffer).
14. Add primary antibodies and incubate overnight at 4°C.
15. Wash 3 x 300 µL PBS for 20-30 sec per step. Leave in PBS while performing next step.
16. Prepare a 200 µL/well solution of secondary antibodies (1:200) in blocking buffer in a 1.5 mL centrifuge tube. DAPI can be used to stain nuclei (1:1000).
17. Apply secondary antibody solution to the organoids, and incubate for 1 h at RT. Cover the plate with aluminium foil to protect from light.
18. Wash 3 x in 300 µL PBS 20-30 sec per step. CRITICAL STEP Maintain in PBS for storage and imaging.

    PAUSE POINT Stained organoids may be stored in PBS at 4°C protected from light for no more than 2 weeks.

19. Proceed to step 40 option B of the main Procedure.

- **END OF BOX 1 -**

Mounting and imaging.

CRITICAL Samples cleared with FLASH can be imaged both with confocal microscopy (CM) and light-sheet microscopy (LSM). Both types of microscopy have benefits and limitations and it is important to choose the right imaging approach according to the experimental needs. A guide with considerations about the advantages and drawbacks can be found in Supplementary Methods.

40. For imaging whole tissues and embryos using light-sheet microscopy (LSFM), follow Option A. For cellular and subcellular resolution imaging using confocal microscopy, follow Option B.

Option A: Imaging in LSFM (for large tissue samples) Timing 10-30 min per organ**:**

i. Initiate the microscope, camera, lasers and computer.

ii. Place the protective dipping cap on the detection lens.

iii. Fill the imaging chamber with MetSal or BABB 100%.

iv. Mount the sample in the sample holder. LaVision BioTec offers different alternatives. Either directly pin the sample to a metal plug or restrain the sample with a screw.

! CRITICAL STEP When the sample is pinned to a metal plug, the plugs will be visible in the 3D reconstructions. To avoid it, embed the sample in 1% (wt/vol) agarose and perform the dehydration and clearing of the entire agarose block. Pin the agarose block making sure the plugs do not reach the tissue.

v. Carefully place the sample holder in the imaging chamber, immersing the sample completely in MetSal or BABB.

vi. Acquire images. Acquisition parameters vary between samples. for our acquisitions we used 200 ms exposure time, double side illumination, 10 μm z-step, 100% light-sheet width and Blend mode. Laser intensity, zoom factor, thickness and waist position were adjusted for each sample. When imaging large volumes that require stitching, take Z-stacks with an overlap of 15% or higher between tiles.

? TROUBLESHOOTING

Option B: Imaging in confocal microscope (for subcellular resolution in tissue or organoids). Timing 5-15 min per stack with a dry objective. 30 min – 1 h per z-stack with immersion objective.

i. Mount the cleared tissue in MetSal or BABB, between two coverglasses. Organoids prepared in Box 1 may be imaged directly immersed in PBS in the chamber slide.

! CAUTION MetSal melts certain plastics. Glass-bottom tissue culture dishes cannot be used for mounting. We recommend using a large coverslip (4 x 6 cm) as a bottom “slide” and covering the tissue with a smaller coverslip. This is a fragile support for the tissue, and extra care should be taken to avoid MetSal dripping on any microscope parts. For

increased security, a custom sample holder can be 3D-printed in MetSal resistant plastic or in metal and the bottom slide attached with MetSal resistant superglue (Fig. 1).

ii. Image Z-stack[58]. Use a live scan to set upper and lower boundaries for Z-stack acquisition, ensuring the boundaries are well outside the sample volume of interest. Allow the software to automatically select the appropriate number of slices needed to image the sample volume, given the axial resolution of the objective and pinhole diameter. When imaging large volumes that require stitching, take Z-stacks with an overlap of 15% or higher between tiles.

? TROUBLESHOOTING

Image processing, 3D rendering and analysis. Timing variable.

41. Perform manual stitching of the tiles in ImageJ with the BigStitcher plugin[56]. Alternatively, use the TeraStitcher plugin[57] available in the LaVision BioTec acquisition software (ImSpector Pro).
42. Perform 3D rendering in ImageJ or directly convert the z-stack into Imaris using Imaris Converter.
43. Perform data analysis, 3D cropping, and capture of optical sections and representative images as needed in Imaris.

(Optional) Conventional histopathology

CRITICAL After imaging, cleared samples can be used for conventional histopathology (staining, IHC and IF).

44. Replace the MetSal with EtOH by placing samples in 10-50 mL each of 75%-50%-25% (vol/vol) MetSal in EtOH, 30 min per step at RT.
45. Place samples in 100% EtOH.

    PAUSE POINT Keep samples in 100% EtOH at 4°C for up to 1 week.
46. Proceed for conventional histology as normal (paraffin embedding, microtome cutting, etc.)[45].

    ? TROUBLESHOOTING

Timing

Box 1, organoid fixation, antigen retrieval and staining: 1 d.

Steps 1-12, vascular stain, collection and fixation: 1 d.

Steps 13-26, dissection and antigen retrieval: 1 d.

Steps 27-34, blocking and immunolabelling: 4 d.

Steps 35-39, dehydration and clearing: 5 h.

Step 40 option A, imaging in LSFM: 10-30 min per organ.

Step 40 option B, imaging in confocal microscope: 5-15 min per stack with a dry (non-immersion) objective. 30 min – 1 h per z-stack with immersion objective.

Steps 41-43, tiling, 3D rendering, and data analysis: 30-90 min per organ or confocal z-stack.

Steps 44-46, replace MetSal with EtOH for conventional histology: 1.5 h.

Troubleshooting

Troubleshooting guidance can be found in Table 2.

Table 2. Troubleshooting Table

Step	Problem	Possible Reason	Solution
14	Sample is damaged	Sample handling too harsh	Be gentle during sample procurement
26	Sample is degraded	Antigen retrieval temperature or time too high	Decrease antigen retrieval temperature or time
28	Sample is damaged	Sample handling too harsh	Use milder agitation during all incubation steps
39	Samples are not transparent and have a cloudy appearance	Samples were not completely dehydrated before immersion in methyl salicylate	Wash 3x in MetOH before re-immersing in methyl salicylate. Make sure that these steps are performed in a dry environment and at RT
40	High background	Residual blood in the sample	Perfuse mice with PBS before organ procurement, or bleach samples
40	Antibody does not work at all, although it works in IF on tissue sections	Overfixation	Reduce fixation time
40	Sample appears degraded under the microscope	Underfixation	Increase fixation time
40	Antibody gives more noise than in IF on tissue sections	Dirty samples	Clean samples carefully before antigen retrieval and remove any hairs, intestinal contents, etc
40	Staining worked only in some regions of the sample	Uneven sample treatment	Increase depigmentation and antigen retrieval volumes (50mL for one mouse organ)
40	No positive signal, although the antibody works in IF on tissue sections	Incompatibility with SDS	Use FLASH Reagent2
40	Staining worked only on the sample surface	Incubation times too short or antibody volumes too small	Increase incubation times and/or antibody volume

40	High background	Low specificity of the primary antibody	Check antibody specificity in IF on tissue sections. Any background, even if in another tissue layer like adjacent blood vessels, can compromise 3D appearance if those structures are very abundant (E.g. blood vessels that appear adjacent to a group of cells in 2D actually surround them in 3D which masks the cells' presentation in the 3D reconstruction)
40	Antibody gives more noise than in IF on tissue sections	Secondary antibody precipitates	Filter any secondary antibodies that precipitate
40	DNA stain did not work	Dye incompatible with FLASH or RI-matching medium	Use another dye. In our hands DRAQ5, propidium iodide and Hoechst33342 work well with FLASH Reagent1. DRAQ5, Hoechst33342 and DAPI work well with FLASH Reagent2
40	Light does not penetrate the tissue	The staining cannot be seen in deeper layers due to extensive light scattering	Use long wavelength secondary antibodies
46	Histological staining faint	Incompatibility with SDS	Use Flash Reagent2

Anticipated results

In this protocol we describe FLASH, a simple and versatile approach allowing for imaging of disparate samples including different organs of the adult mouse (Figs. 2-5; Supplementary Videos 1-6), human biopsies (Fig. 4d), other organisms such as *Drosophila melanogaster* (Fig. 5c), organoids (Fig. 6), and mouse embryos (Fig. 8; Supplementary Video 7). FLASH preserves the integrity of the tissue, and allows imaging with cellular and subcellular resolution. Since FLASH-imaged tissues and organisms remain intact, the technique can be fully integrated into standard histopathology workflows, enhancing its versatility and providing a rigorous way of validating the 3D-imaging observations (Fig. 2d-f).

We previously used FLASH to quantify the relative deformations of cancerous tubular epithelia in the pancreas, liver and lung[1]. FLASH can be used to study morphometric characteristics of adenocarcinoma progression with subcellular resolution, as shown in KrasG12D$^{+/-}$ TP53$^{F/F}$ Pdx1-Cre mice bearing cancerous lesions (Fig. 7a), the tumour niche, including the abnormal vasculature in PDAC (Fig. 7b), whole tumour growth as shown in the entire mammary gland of MMTV-PyMT mice (Fig. 7c), and total metastatic lesions, exemplified in lungs of MMTV-PyMT mice and mice injected intravenously with 4T1 mammary cancer cells (Fig. 7 d, e).

Recently, we applied FLASH to investigate the machinery driving cytokinetic abscission in mice[2]. We used FLASH to characterize whole mouse embryos lacking the abscission regulator Cep55, and identified aberrant apoptosis specifically in the central and peripheral nervous systems (Fig. 8a)[61]. FLASH on a variety of dissected

embryonic organs allowed us to visualize and quantify intercellular bridges that connect dividing cells at the end of mitosis in $Cep55^{+/+}$ and $Cep55^{-/-}$ embryos (Fig. 8b).

Thus, FLASH constitutes a rapid and robust protocol for 3D immunofluorescence, which has already been applied to investigate molecular mechanisms in cancer initiation and cell division in development. We are working to expand its reach, answering questions in neuroscience, immunology and clinical research, and anticipate that it may be useful across an even broader range of research questions.

Figure legends:

Figure 1. **Overview of FLASH**. The protocol is divided into the full (1-week) workflow for tissue samples (mouse organs and biopsies, steps 1-39 of the procedure) and the condensed (1-day) workflow for organoids (Box 1). For the full workflow, after vasculature labelling and organ collection (steps 1-12), samples are fixed, microdissected under a stereomicroscope and depigmented as required (steps 13-23). The antigen retrieval solution is selected based on the nature of the tissue and antigen, as well as the downstream image magnification desired (steps 24-26). Samples are then stained, dehydrated and cleared (steps 27-39). Images of whole organs and embryos are acquired in a LSFM (step 40, option A), and cellular and subcellular resolution is achieved with a confocal microscope (step 40, option B). Z-stacks are tiled, rendered and analysed (steps 41-43). After imaging, samples may be used for conventional histopathology (steps 44-46).

Figure 2. **FLASH enables 3D IF and preserves tissue integrity. a)** Mouse Pancreas transparency before and after FLASH. **b)** 3D views of comparative IF of pancreata incubated in PBS (control, left) or treated with FLASH Reagent1 (middle). Conventional 2D staining on cut sections (right) serves as staining reference. Immunostaining for amylase (acinar cells), PCSK1 (islets of Langerhans), and a-smooth muscle actin (stroma and vasculature). **c)** 3D IF of tyrosine hydroxylase (TH, neurons) in mouse brain incubated in PBS (control, above) or treated with FLASH Reagent1 (below). **d-f)** Haematoxylin and eosin (H&E) staining of pancreas (d), liver (e) and lung (f) treated with PBS or FLASH Reagent2. Tissues were paraffin-

embedded after treatment and processed for conventional 2D staining and histological analysis. All scale bars (b-f), 100 µm, refer to the centre of the 3D views.

Figure 3. **FLASH of lung, stomach, pancreas and mammary gland. a)** FLASH Reagent1 staining of mouse lung for CC10 (club cells), SMA (stroma and vasculature), and SFTPC (alveolar type II cells). $\mathbf{a_i}$ shows the bronchiolar tree of a whole lung lobe (scale bar 1 mm). $\mathbf{a_{ii}}$ is a magnification of the volume indicated in $\mathbf{a_i}$ (scale bar 500 µm). $\mathbf{a_{iii}}$ is a magnified optical section of the volume indicated in $\mathbf{a_{ii}}$ (scale bar 50 µm). $\mathbf{a_{iv}}$ shows a conventional tissue section IF for comparison (scale bar 50 µm). $\mathbf{a_{v,\ vi}}$ show bronchiolar endings and alveoli (scale bars 100 µm). Star indicates bronchiolar lumen. Arrowheads demarcate vessels. Arrows point at bronchus-associated myofibroblasts. **b)** FLASH Reagent1 staining of mouse stomach for Cdh1 (epithelial cells), GIF (murine chief cells), H^+/K^+ ATPase (parietal cells), Muc1 and Muc5AC (glandular units). $\mathbf{b_i}$ shows a view of the stomach at the limiting ridge (dotted line; scale bar 200 µm). $\mathbf{b_{ii,\ iii}}$ show a high magnification of the glandular stomach showing regional separation of chief cells and parietal cells (scale bars 50 and 20 µm). $\mathbf{b_{iv}}$ 3D view of the antrum showing glandular units (scale bar 50 µm). **c)** FLASH Reagent2 staining of mouse pancreas for amylase (cytoplasm of acinar cells) and Mist1 (nuclei of acinar cells) showing acini between sheets of collV (basal lamina). $\mathbf{c_{ii}}$ shows a magnified optical section of the volume shown in $\mathbf{c_i}$. $\mathbf{c_{iii}}$ shows a conventional tissue section IF for comparison. $\mathbf{c_{iv}}$ and $\mathbf{c_v}$ show intensity profiles of the fluorophores in $\mathbf{c_{ii}}$ and $\mathbf{c_{iii}}$ respectively. **d)** FLASH Reagent1 staining of mouse mammary gland for Krt8 (luminal epithelial cells), Krt5 (myoepithelial cells), ColIV (basal lamina) and RFP ($Lgr6^+$ progenitor cells in Lgr6-EGFP-IRES-CreERT2; Rosa26-LSL-tdTomato tamoxifen-treated mice[62,63]). $\mathbf{d_i}$ shows a whole mammary gland of an adult virgin female mouse (scale bar 2 mm). $\mathbf{d_{ii\text{-}vi}}$ show the epithelial structure of ducts in adult virgin female mice (scale bars 20, 10, 100, 50 and 50 µm). $\mathbf{d_{vii}}$ shows a conventional tissue section IF for comparison (scale bar 20 µm). $\mathbf{d_{viii}}$ shows mammary alveoli in the whole mammary gland of an 18-days pregnant female (scale bar 1 mm). Stars indicate mammary duct lumen. All scale bars refer to the centre of the 3D views.

Figure 4. **FLASH of liver, lacrimal gland, kidney and human biopsies. a)** FLASH Reagent1 staining of mouse liver and biliary tree for GS (pericentral hepatocytes),

S100 (nerves), Krt19, DBA and CD44 (bile ducts), SMA (stroma and vasculature), Prox1 (nuclei of lymphatic endothelial cells) and Aqp1 (microvasculature). **a_{i-iii}** show 3D views of hepatic tissue compartments (scale bar 300, 200 and 200 µm). **a_{iv}** shows an optical section of the indicated volume in **a_{iii}** (scale bar 50 µm). **a_{v}** shows a conventional tissue section IF for comparison (scale bar 50 µm). Stars in **$a_{iv, v}$** indicate duct lumen, and arrowheads indicate DBA^+ and DBA^- duct cells. **a_{vi-x}** show extrahepatic bile duct, where stars indicate bile duct lumen, arrows indicate main pancreatic duct and arrowheads indicate peribiliary glands (scale bars 50, 20, 100, 200, and 200 µm). **b)** FLASH Reagent1 staining of mouse lacrimal gland for Krt19 (tear duct cells), SMA (stroma), Aqp1 (microvasculature), vimentin (fibroblasts), S100 (nerves) and Krt14 (myofibroblasts) (scale bars 200, 200, 100, 200 and 100 µm). **c)** FLASH Reagent2 staining of mouse kidney for DBA (collecting ducts and tubules), PNA (distal tubules) and WT1 (nuclei of glomerular cells). **c_{i}** shows renal medulla and cortex (scale bar 1 mm). **c_{ii}** shows glomeruli in the cortex (scale bar 100 µm). **c_{iii}** is an optical section of the volume indicated in **c_{ii}** (scale bar 50 µm). **c_{iv}** shows a conventional tissue section IF for comparison (scale bar 50 µm). **d)** FLASH Reagent1 staining of human pancreas for MUC5A, CDH1 (epithelial cells) and autofluorescence (AF; extracellular matrix). **d_{i-iii}** Ductal metaplasia. **d_{iv-vi}** Intraductal papillary mucinous neoplasia (IPMN) (scale bars 200, 200, 200, 100, 100 and 100 µm). Scale bars refer to the centre of the 3D views.

Figure 5. **FLASH of highly pigmented tissues. a)** Heart transparency before and after depigmentation and FLASH. **b)** Immunofluorescence by FLASH Reagent2 of whole mouse heart for TH (nerves) and ColIV (extracellular matrix) (scale bar 700 µm). **c)** Immunofluorescence by FLASH Reagent1 of 500 µm heart slices for TH and ColIV (scale bars 50 and 20 µm). **d)** Immunofluorescence by FLASH Reagent1 of whole mouse heart for CD31 (vasculature) and ColIV (scale bars 50 µm). **e)** Spleen transparency before and after depigmentation and FLASH. **f)** Immunofluorescence by FLASH Reagent1 of whole mouse spleen for CD3 (T cells), B220 (B cells) and CD16 (natural killer cells, neutrophils and macrophages) (scale bars 1.5 mm and 100 µm). **g)** FLASH Reagent1 staining of a UASStingerGFP/+; R2R4Gal4^{64}/+ *Drosophila melanogaster* for GFP (nuclei of R2 and R4 enterocytes) treated with PBS (control) or 35% H_2O_2 before antigen retrieval (scale bars 100 µm). Scale bars refer to the centre of the 3D views.

Figure 6. **FLASH of MMTV-PyMT organoids. a)** Comparative IF of organoids treated with PBS (control) or FLASH Reagent2, showing Ki67 (nuclear puncta in proliferative cells) and DAPI (nuclei) staining (scale bars 10 µm). **b)** Comparative IF of organoids treated with PBS (control) or FLASH Reagent2, showing PCNA (nuclear puncta in proliferative cells) (scale bars 7 µm). **c)** FLASH Reagent2 staining of an organoid for AurB (midbody), PCNA and DAPI (scale bars 10 and 3 µm). Scale bars refer to the centre of the 3D views.

Figure 7. **FLASH for characterising epithelial pathophysiology. a)** FLASH Reagent1 staining of pancreatic neoplastic lesions for Krt19 (epithelial cells) and DRAQ5 (nuclei) in the KrasG12D$^{+/-}$ TP53$^{F/F}$ Pdx1-Cre (KPC) model of PDAC. **a_i** shows a three-dimensional reconstruction of Krt19-stained pancreas from a three-week-old KPC mouse with multiple neoplastic tissue alterations (scale bar 300 µm). **$a_{ii,iv}$** are high magnifications of the regions indicated in **a_i** (scale bars 50 µm). **a_{iii}** is an optical section through the indicated area in **a_{ii}**, showing endophytically[1] deformed ductal epithelium and columnar cells with nuclear expansion (scale bar 25 µm). **a_v** is an optical section through the indicated area in **a_{iv}**, showing an exophytic[1] lesion (scale bar 25 µm). **b)** FLASH Reagent1 staining of abnormal vasculature in early PDAC with Lectin 594 (scale bar 70 µm). **c)** FLASH Reagent1 staining of entire mammary glands and tumours for Krt8 (luminal epithelial cells) in MMTV-PyMT mice of 6 and 11 weeks of age (scale bars 1.5 mm and 500 µm). **d)** FLASH Reagent1 staining of spontaneous metastatic lesions in lungs of MMTV-PyMT mice for Krt8 (luminal epithelial cells), Pdpn (alveolar cells), SMA (stroma and vasculature) and SFTPC (type I alveolar cells) (scale bars 1 mm, 50 and 25 µm). **e)** Mammary macrometastases in whole lungs of a mouse injected with 4T1 cells intravenously 2 weeks prior to euthanasia (scale bar 300 µm). Scale bars refer to the centre of the 3D views.

Figure 8. **FLASH for studying embryonic development. a)** FLASH Reagent2 staining of wildtype and Cep55$^{-/-}$ E13.5 embryos for CC3 (apoptotic cells). Autofluorescence (AF) delineates the volume of the embryos (scale bars 1 mm and 500 µm). **b)** FLASH Reagent2 staining of a lung of an E18.5 Cep55$^{-/-}$ embryo for Tub

and AurB (intercellular bridge) and DAPI (nuclei). Yellow circle indicates intercellular bridge (scale bars 10 µm). Scale bars refer to the centre of the 3D views.

References

1 Messal, H. A. *et al.* Tissue curvature and apicobasal mechanical tension imbalance instruct cancer morphogenesis. *Nature* **566**, 126-130, doi:10.1038/s41586-019-0891-2 (2019).

2 Tedeschi, A. *et al.* Cep55 promotes cytokinesis of neural progenitors but is dispensable for most mammalian cell divisions. *Nat Commun* **11**, 1746, doi:10.1038/s41467-020-15359-w (2020).

3 Huisken, J., Swoger, J., Del Bene, F., Wittbrodt, J. & Stelzer, E. H. Optical sectioning deep inside live embryos by selective plane illumination microscopy. *Science* **305**, 1007-1009, doi:10.1126/science.1100035 (2004).

4 Ueda, H. R. *et al.* Tissue clearing and its applications in neuroscience. *Nat Rev Neurosci* **21**, 61-79, doi:10.1038/s41583-019-0250-1 (2020).

5 Richardson, D. S. & Lichtman, J. W. Clarifying Tissue Clearing. *Cell* **162**, 246-257, doi:10.1016/j.cell.2015.06.067 (2015).

6 Dekkers, J. F. *et al.* High-resolution 3D imaging of fixed and cleared organoids. *Nat Protoc* **14**, 1756-1771, doi:10.1038/s41596-019-0160-8 (2019).

7 Sachs, N. *et al.* Long-term expanding human airway organoids for disease modeling. *The EMBO journal* **38**, doi:10.15252/embj.2018100300 (2019).

8 Hu, H. *et al.* Long-Term Expansion of Functional Mouse and Human Hepatocytes as 3D Organoids. *Cell* **175**, 1591-1606 e1519, doi:10.1016/j.cell.2018.11.013 (2018).

9 Susaki, E. A. *et al.* Advanced CUBIC protocols for whole-brain and whole-body clearing and imaging. *Nat Protoc* **10**, 1709-1727, doi:10.1038/nprot.2015.085 (2015).

10 Susaki, E. A. *et al.* Whole-brain imaging with single-cell resolution using chemical cocktails and computational analysis. *Cell* **157**, 726-739, doi:10.1016/j.cell.2014.03.042 (2014).

11 Chung, K. *et al.* Structural and molecular interrogation of intact biological systems. *Nature* **497**, 332-337, doi:10.1038/nature12107 (2013).

12 Tainaka, K. *et al.* Whole-body imaging with single-cell resolution by tissue decolorization. *Cell* **159**, 911-924, doi:10.1016/j.cell.2014.10.034 (2014).

13 Matsumoto, K. *et al.* Advanced CUBIC tissue clearing for whole-organ cell profiling. *Nat Protoc* **14**, 3506-3537, doi:10.1038/s41596-019-0240-9 (2019).

14 Tainaka, K. *et al.* Chemical Landscape for Tissue Clearing Based on Hydrophilic Reagents. *Cell Rep* **24**, 2196-2210 e2199, doi:10.1016/j.celrep.2018.07.056 (2018).

15 Murakami, T. C. *et al.* A three-dimensional single-cell-resolution whole-brain atlas using CUBIC-X expansion microscopy and tissue clearing. *Nat Neurosci* **21**, 625-637, doi:10.1038/s41593-018-0109-1 (2018).

16 Cai, R. *et al.* Panoptic imaging of transparent mice reveals whole-body neuronal projections and skull-meninges connections. *Nat Neurosci* **22**, 317-327, doi:10.1038/s41593-018-0301-3 (2019).

17 Cai, R. *et al.* Panoptic vDISCO imaging reveals neuronal connectivity, remote trauma effects and meningeal vessels in intact transparent mice. doi:10.1101/374785 (2018).

18 Pan, C. *et al.* Deep Learning Reveals Cancer Metastasis and Therapeutic Antibody Targeting in the Entire Body. *Cell* **179**, 1661-1676 e1619, doi:10.1016/j.cell.2019.11.013 (2019).

19 Zhao, S. *et al.* Cellular and Molecular Probing of Intact Human Organs. *Cell* **180**, 796-812 e719, doi:10.1016/j.cell.2020.01.030 (2020).

20 Chen, B. C. *et al.* Lattice light-sheet microscopy: imaging molecules to embryos at high spatiotemporal resolution. *Science* **346**, 1257998, doi:10.1126/science.1257998 (2014).

21 Camacho, D. M., Collins, K. M., Powers, R. K., Costello, J. C. & Collins, J. J. Next-Generation Machine Learning for Biological Networks. *Cell* **173**, 1581-1592, doi:10.1016/j.cell.2018.05.015 (2018).

22 Sullivan, D. P. *et al.* Deep learning is combined with massive-scale citizen science to improve large-scale image classification. *Nature biotechnology* **36**, 820-828, doi:10.1038/nbt.4225 (2018).

23 Wang, H. *et al.* Deep learning enables cross-modality super-resolution in fluorescence microscopy. *Nat Methods* **16**, 103-110, doi:10.1038/s41592-018-0239-0 (2019).

24 Todorov, M. I. *et al.* Machine learning analysis of whole mouse brain vasculature. *Nat Methods* **17**, 442-449, doi:10.1038/s41592-020-0792-1 (2020).

25 Erturk, A. *et al.* Three-dimensional imaging of solvent-cleared organs using 3DISCO. *Nat Protoc* **7**, 1983-1995, doi:10.1038/nprot.2012.119 (2012).

26 Erturk, A. *et al.* Three-dimensional imaging of the unsectioned adult spinal cord to assess axon regeneration and glial responses after injury. *Nature medicine* **18**, 166-171, doi:10.1038/nm.2600 (2012).

27 Yang, B. *et al.* Single-cell phenotyping within transparent intact tissue through whole-body clearing. *Cell* **158**, 945-958, doi:10.1016/j.cell.2014.07.017 (2014).

28 Renier, N. *et al.* iDISCO: a simple, rapid method to immunolabel large tissue samples for volume imaging. *Cell* **159**, 896-910, doi:10.1016/j.cell.2014.10.010 (2014).

29 Belle, M. *et al.* Tridimensional Visualization and Analysis of Early Human Development. *Cell* **169**, 161-173 e112, doi:10.1016/j.cell.2017.03.008 (2017).

30 Murray, E. *et al.* Simple, Scalable Proteomic Imaging for High-Dimensional Profiling of Intact Systems. *Cell* **163**, 1500-1514, doi:10.1016/j.cell.2015.11.025 (2015).

31 Pan, C. *et al.* Shrinkage-mediated imaging of entire organs and organisms using uDISCO. *Nat Methods* **13**, 859-867, doi:10.1038/nmeth.3964 (2016).

32 Kubota, S. I. *et al.* Whole-Body Profiling of Cancer Metastasis with Single-Cell Resolution. *Cell Rep* **20**, 236-250, doi:10.1016/j.celrep.2017.06.010 (2017).

33 Forbes, R. M., Cooper, A. R. & Mitchell, H. H. The composition of the adult human body as determined by chemical analysis. *The Journal of biological chemistry* **203**, 359-366 (1953).

34 McIlwain, H. & Bachelard, H. S. *Biochemistry and the central nervous system*. (Curchill Livingstone, 1985).

35 Shi, S. R., Cote, R. J. & Taylor, C. R. Antigen retrieval techniques: current perspectives. *J Histochem Cytochem* **49**, 931-937, doi:10.1177/002215540104900801 (2001).

36 Tomer, R., Ye, L., Hsueh, B. & Deisseroth, K. Advanced CLARITY for rapid and high-resolution imaging of intact tissues. *Nat Protoc* **9**, 1682-1697, doi:10.1038/nprot.2014.123 (2014).

37 Tillberg, P. W. *et al.* Protein-retention expansion microscopy of cells and tissues labeled using standard fluorescent proteins and antibodies. *Nature biotechnology* **34**, 987-992, doi:10.1038/nbt.3625 (2016).

38 Kim, S. H., Kook, M. C., Shin, Y. K., Park, S. H. & Song, H. G. Evaluation of antigen retrieval buffer systems. *J Mol Histol* **35**, 409-416, doi:10.1023/b:hijo.0000039854.17808.e0 (2004).

39 White, L. J. *et al.* The impact of detergents on the tissue decellularization process: A ToF-SIMS study. *Acta Biomater* **50**, 207-219, doi:10.1016/j.actbio.2016.12.033 (2017).

40 Brito, R. M. & Vaz, W. L. Determination of the critical micelle concentration of surfactants using the fluorescent probe N-phenyl-1-naphthylamine. *Analytical biochemistry* **152**, 250-255, doi:10.1016/0003-2697(86)90406-9 (1986).

41 Midura, R. J. & Yanagishita, M. Chaotropic solvents increase the critical micellar concentrations of detergents. *Analytical biochemistry* **228**, 318-322, doi:10.1006/abio.1995.1357 (1995).

42 Hama, H. *et al.* Scale: a chemical approach for fluorescence imaging and reconstruction of transparent mouse brain. *Nat Neurosci* **14**, 1481-1488, doi:10.1038/nn.2928 (2011).

43 Ke, M. T., Fujimoto, S. & Imai, T. SeeDB: a simple and morphology-preserving optical clearing agent for neuronal circuit reconstruction. *Nat Neurosci* **16**, 1154-1161, doi:10.1038/nn.3447 (2013).

44 Coutu, D. L., Kokkaliaris, K. D., Kunz, L. & Schroeder, T. Multicolor quantitative confocal imaging cytometry. *Nat Methods* **15** (2018).

45 Slaoui, M. & Fiette, L. Histopathology procedures: from tissue sampling to histopathological evaluation. *Methods Mol Biol* **691**, 69-82, doi:10.1007/978-1-60761-849-2_4 (2011).

46 Li, W., Germain, R. N. & Gerner, M. Y. High-dimensional cell-level analysis of tissues with Ce3D multiplex volume imaging. *Nat Protoc* **14**, 1708-1733, doi:10.1038/s41596-019-0156-4 (2019).

47 Hamers-Casterman, C. *et al.* Naturally occurring antibodies devoid of light chains. *Nature* **363**, 446-448, doi:10.1038/363446a0 (1993).

48 Arbabi-Ghahroudi, M. Camelid Single-Domain Antibodies: Historical Perspective and Future Outlook. *Front Immunol* **8**, 1589, doi:10.3389/fimmu.2017.01589 (2017).

49 Fang, T. *et al.* Nanobody immunostaining for correlated light and electron microscopy with preservation of ultrastructure. *Nat Methods* **15**, 1029-1032, doi:10.1038/s41592-018-0177-x (2018).

50 Susaki, E. A. *et al.* Versatile whole-organ/body staining and imaging based on electrolyte-gel properties of biological tissues. *Nat Commun* **11**, 1982, doi:10.1038/s41467-020-15906-5 (2020).

51 Hama, H. *et al.* ScaleS: an optical clearing palette for biological imaging. *Nat Neurosci* **18**, 1518-1529, doi:10.1038/nn.4107 (2015).

52 Zhao, Y. *et al.* Nanoscale imaging of clinical specimens using pathology-optimized expansion microscopy. *Nature biotechnology* **35**, 757-764, doi:10.1038/nbt.3892 (2017).

53 Chen, F., Tillberg, P. & Boyden, E. Expansion microscopy. *Science* **347**, 543-548 (2015).

54 Shen, K., Sun, J., Cao, X., Zhou, D. & Li, J. Comparison of Different Buffers for Protein Extraction from Formalin-Fixed and Paraffin-Embedded Tissue Specimens. *PloS one* **10**, e0142650, doi:10.1371/journal.pone.0142650 (2015).

55 Schindelin, J. *et al.* Fiji: an open-source platform for biological-image analysis. *Nat Methods* **9**, 676-682, doi:10.1038/nmeth.2019 (2012).

56 Horl, D. *et al.* BigStitcher: reconstructing high-resolution image datasets of cleared and expanded samples. *Nat Methods* **16**, 870-874, doi:10.1038/s41592-019-0501-0 (2019).

57 Bria, A. & Iannello, G. TeraStitcher - a tool for fast automatic 3D-stitching of teravoxel-sized microscopy images. *BMC Bioinformatics* **13**, 316, doi:10.1186/1471-2105-13-316 (2012).

58 Jonkman, J., Brown, C. M., Wright, G. D., Anderson, K. I. & North, A. J. Guidance for quantitative confocal microscopy. *Nat Protoc*, doi:10.1038/s41596-020-0307-7 (2020).

59 Smolla, M., Ruchty, M., Nagel, M. & Kleineidam, C. J. Clearing pigmented insect cuticle to investigate small insects' organs in situ using confocal laser-scanning microscopy (CLSM). *Arthropod Struct Dev* **43**, 175-181, doi:10.1016/j.asd.2013.12.006 (2014).

60 Guy, C. T., Cardiff, R. D. & Muller, W. J. Induction of mammary tumors by expression of polyomavirus middle T oncogene: a transgenic mouse model for metastatic disease. *Molecular and cellular biology* **12**, 954-961, doi:10.1128/mcb.12.3.954 (1992).

61 Carlton, J. G. & Martin-Serrano, J. Parallels between cytokinesis and retroviral budding: a role for the ESCRT machinery. *Science* **316**, 1908-1912, doi:10.1126/science.1143422 (2007).

62 Snippert, H. J. *et al.* Lgr6 Marks Stem Cells in the Hair Follicle That Generate All Cell Lineages of the Skin. *Science* **327** (2010).

63 Blaas, L. *et al.* Lgr6 labels a rare population of mammary gland progenitor cells that are able to originate luminal mammary tumours. *Nat Cell Biol* **18**, 1346-1356, doi:10.1038/ncb3434 (2016).

64 Hudry, B. *et al.* Sex Differences in Intestinal Carbohydrate Metabolism Promote Food Intake and Sperm Maturation. *Cell* **178**, 901-918 e916, doi:10.1016/j.cell.2019.07.029 (2019).

Acknowledgments

We thank C. Cremona for comments on the manuscript, I. Evans for support with supplies, J. Brock, research illustration, for editing Supplementary Video 7 and the Francis Crick Institute Biological Research, Experimental Histopathology and Advanced Light Microscopy facilities for technical assistance. This work was supported by the Francis Crick Institute, which receives its core funding from Cancer Research UK (FC001039), the UK Medical Research Council (FC001039) and the Wellcome Trust (FC001039). This work was also financially supported by the European Molecular Biology Organization (EMBO long-term fellowship ALTF 452-2019 to H.A.M.), the European Research Council (ERC consolidator grant 648804 to J.v.R.), the Doctor Josef Steiner Foundation (to J.v.R.) and the European Research Council (ERC grant 281661 to A.B.).

Author contributions

H.A.M. conceived and developed the protocol. J.A. contributed to the development of the protocol. H.A.M. and J.A. cowrote this manuscript. M.Z.T. contributed to the comparison with other 3D IF methods, the development of the adaptation for pigmented tissue and performed vasculature labelling in tumour models. A.T. isolated embryos and embryonic tissues, and contributed with the experimental design and analysis of intercellular bridges in 3D. M.Z.T. and A.T. contributed equally. A.C. and K.I.A. provided support with microscopy. L.B. developed the adaptation for insect clearing. I.M.A., J.v.R. and A.B. supervised the project. All authors read and contributed to the correction of the manuscript.

Competing interests

H.A.M. and A.B. are inventors on a UK patent application (1818567.8) relating to solutions for preparation of samples for 3D imaging.

Data availability

The raw image files used to obtain Figures 2-8, Extended Data Figures 1-9 and Supplementary Videos 1-6 are available from the corresponding author upon reasonable request. Data in Supplementary Video 7 corresponds to the whole embryo samples imaged by FLASH for the paper by Tedeschi and colleagues[2].

Related Links

1. Messal, H. A. *et al.* Tissue curvature and apicobasal mechanical tension imbalance instruct cancer morphogenesis. *Nature* **566**, 126-130 (2019). https://www.nature.com/articles/s41586-019-0891-2
2. Tedeschi, A. *et al.* Cep55 promotes cytokinesis of neural progenitors but is dispensable for most mammalian cell divisions. *Nat Commun* **11**, 1746 (2020). https://www.nature.com/articles/s41467-020-15359-w

Supplementary information

Extended Data Figure Legends

Extended Data Figure 1. **Influence of buffer, pH, temperature and detergent on antigen retrieval. a)** Whole pancreatic lobules were treated for 16 hrs with the indicated buffers containing 4% (wt/vol) SDS at the indicated temperatures. Shown are representative stainings for Krt19 (pancreatic ducts). Blue lines indicate minimum temperature above which staining was observed; red lines indicate maximum temperature above which sample damage was noted. Crosses indicate sample loss. **b)** 3D view of a pancreatic lobule after cardiac perfusion with dextran-FITC before and after FLASH Reagent1 treatment (scale bar 150 µm). **c)** Comparative whole pancreas immunolabeling for keratin 19 (ducts), C-peptide (islets of Langerhans) and amylase (acinar cells). Samples were incubated at 54degC with borate alone (left column) and borate with the indicated detergents (all 8% wt/vol) without urea. All scale bars 300 µm.

Extended Data Figure 2. **FLASH Reagent2 preserves the integrity of cytoskeleton and embryos. a, b)** Comparative 3D IF of 100 µm mouse liver sections treated with FLASH Reagent1 or Reagent 2. Immunostaining for a-tubulin (tubulin cytoskeleton; a) and cytochrome P450 (microsomes, b). Nuclei were stained with DRAQ5. Scale bars 7 µm (a) and 5 µm (b). **c)** Images of E13.5 embryos after

antigen retrieval with FLASH Reagent1 and Reagent2. **d)** Comparative IF of 100 µm mouse lung slices treated with FLASH Reagent1 or Reagent2. Immunostaining for a-tubulin and acetylated tubulin (ac-tubulin; cilia of bronchiolar epithelia). Nuclei were stained with DRAQ5. Scale bars 50 µm (top panels), 5 µm (centre; 4 panels) and 2 µm (bottom panels).

Extended Data Figure 3. **FLASH compatibility with different RI-matching media. a)** Timeline of sample processing after FLASH staining. BABB (benzyl alcohol/benzyl benzoate), THF (tetrahydrofuran), DCM (dichloromethane), DBE (dibenzyl ether), TdE (thiodiethanol), tB (tert butanol), BABB-D4 (BABB + diphenyl ether). **b)** Representative optical sections showing nuclear staining (Hoechst33342, Dapi) after RI-matching as indicated. All scale bars 50 µm. **c)** Imaging depth for indicated organs and RI-matching media. Note that the tissue depth that can be imaged is not only affected by the optical imaging depth but also by the extent of sample shrinkage/expansion (also see (d)). A deeper imaging depth of expanded tissue (e.g. in CUBIC-treated pancreas) might capture the same number of cell layers as a lower imaging depth on shrunken tissue. **d)** Estimate of nuclear density indicating the effect of RI-media on tissue size as shown for the pancreas. **e)** Signal-to-noise ratio for different organs with the indicated RI-media. **f)** FLASH-compatible mounting media and their approximate RI.

Extended Data Figure 4. **FLASH with fluorophore-conjugated nanobody staining. a)** Scheme of the alleles in the mouse model with GFP-expressing pancreatic cells used in b and c. **b)** 3D IF by standard FLASH (primary and secondary antibodies) labelling GFP (pancreatic cells). **c)** 3D IF of GFP (pancreatic cells) after 1 day (left) or 2 days (right) of labelling with a fluorophore-conjugated anti-GFP nanobody. **d)** Scheme of the alleles in the mouse model with GFP-expressing pancreatic ductal cells used in e and f. **e)** 3D IF by standard FLASH labelling GFP (pancreatic ductal cells). **f)** 3D IF of GFP (pancreatic ductal cells) after 1 day (left) or 2 days (right) of labelling with a fluorophore-conjugated anti-GFP nanobody. **g)** Comparison of required time for standard FLASH and FLASH using a fluorophore-conjugated nanobody. Scale bars 100 µm (b, c) or 50 µm (e, f).

Extended Data Figure 5. **Time and clearing comparison in FLASH (Reagent1) and other methods. a)** Comparison of processing time for each of the methods, from tissue collection to mounting for imaging (see also Extended Data Figures 6-9). **b)** Images of tissues cleared with different methods. Yellow dotted line indicates position of tissue in completely transparent samples.

Extended Data Figure 6. **3D immunofluorescence of brain cortex with FLASH and other methods.** 3D IFs of cortex in 500 µm-thick brain slices with different clearing techniques as indicated, labelling **a)** GFAP (astrocytes), a-SMA (vasculature) and **b)** TH (axons). Scale bars 20 µm.

Extended Data Figure 7. **3D immunofluorescence of pancreata with FLASH and other methods.** 3D IFs of pancreas with different clearing techniques as indicated, labelling **a)** Krt19, TH (nerves), a-SMA (vasculature) and **b)** Krt19 (ductal cells), C-pep (islets of Langerhans), Amy (acinar cells). Scale bars 50 µm.

Extended Data Figure 8. **3D immunofluorescence of mammary glands with FLASH and other methods.** 3D IFs of mammary gland with different clearing techniques as indicated, labelling **a)** Krt8 (luminal cells), a-SMA (myoepithelial cells and vasculature), ColIV (basement membrane), **b)** Krt8, CD31 (endothelial cells) and **c)** FoxP1 (nuclei of mammary gland cells). Scale bars 50 µm (a, b) and 30 µm (c).

Extended Data Figure 9. **Fluorescence intensity and signal-to-noise ratio (SNR) across imaging depth in FLASH and other methods. a)** Stacks of mammary glands imaged after different clearing methods (left and centre panels). Look-Up-Tables (LUTs) of Maximum Intensity Projections (MIPs) of the side views show fluorescent intensity across the tissue depth (right panels). Representative images of 2 independent experiments. Scale bars 100 µm. b) SNR over the imaging depth of the mammary gland with indicated clearing methods. For CUBIC-HistoVIsion, AbScale and SWITCH, no signal could be observed after up to 200 µm. Signal in FLASH and iDISCO treated sampled could be discerned through the whole sample thickness.

Supplementary Methods

Supplementary Table 1, comparison of detergents for antigen retrieval

Supplementary Table 2, selected antibodies and lectins validated for FLASH

Supplementary Table 3, procedure recommendation according to sample type

Supplementary Table 4, comparison of FLASH with other 3D imaging techniques

Supplementary Video Legends

Supplementary Video 1. **FLASH of lung.**

3D confocal image of bronchiole and arteriole (SMA, magenta), Clara Cells (CC10, green) and alveolar type II cells (SFTPC, cyan) in a mouse lung treated with FLASH Reagent1.

Supplementary Video 2. **FLASH of pancreas.**

Confocal image of pancreatic duct (Krt19, white) and islets of Langerhans (PCSK1, red) in a mouse pancreas treated with FLASH Reagent1.

Supplementary Video 3. **FLASH of whole mammary gland.**

Light-sheet image of mammary ducts (Krt8 and Krt5, pink) and basal lamina defining adipocytes (ColIV, beige) of an entire mammary gland of an adult virgin mouse, treated with FLASH Reagent1.

Supplementary Video 4. **FLASH of mammary epithelium.**

Confocal image of a duct in the mammary gland from Supplementary Video 3, showing luminal cells (Krt8, pink), myoepithelial cells (Krt5, yellow) and basal lamina defining adipocytes (ColIV, beige).

Supplementary Video 5. **FLASH of bile duct.**

Confocal image of a murine extrahepatic bile duct (Krt19, cyan) and microvasculature (Aqp1, red) treated with FLASH Reagent1.

Supplementary Video 6. **FLASH of lacrimal gland.**

Confocal image of tear ducts (Krt19, green), microvasculature (Aqp1, yellow) and stroma (SMA, magenta) of a mouse lacrimal gland treated with FLASH Reagent1.

Supplementary Video 7. **FLASH of wildtype and Cep55$^{-/-}$ embryos.**

Light-sheet image of whole E13.5 wildtype and Cep55$^{-/-}$ mouse embryos treated with FLASH Reagent2. Outline of entire embryo (autofluorescence, grey) and apoptotic cells (CC3, red). Images of the embryos in this video were included in a previous publication from our laboratory[2].

Figure 1

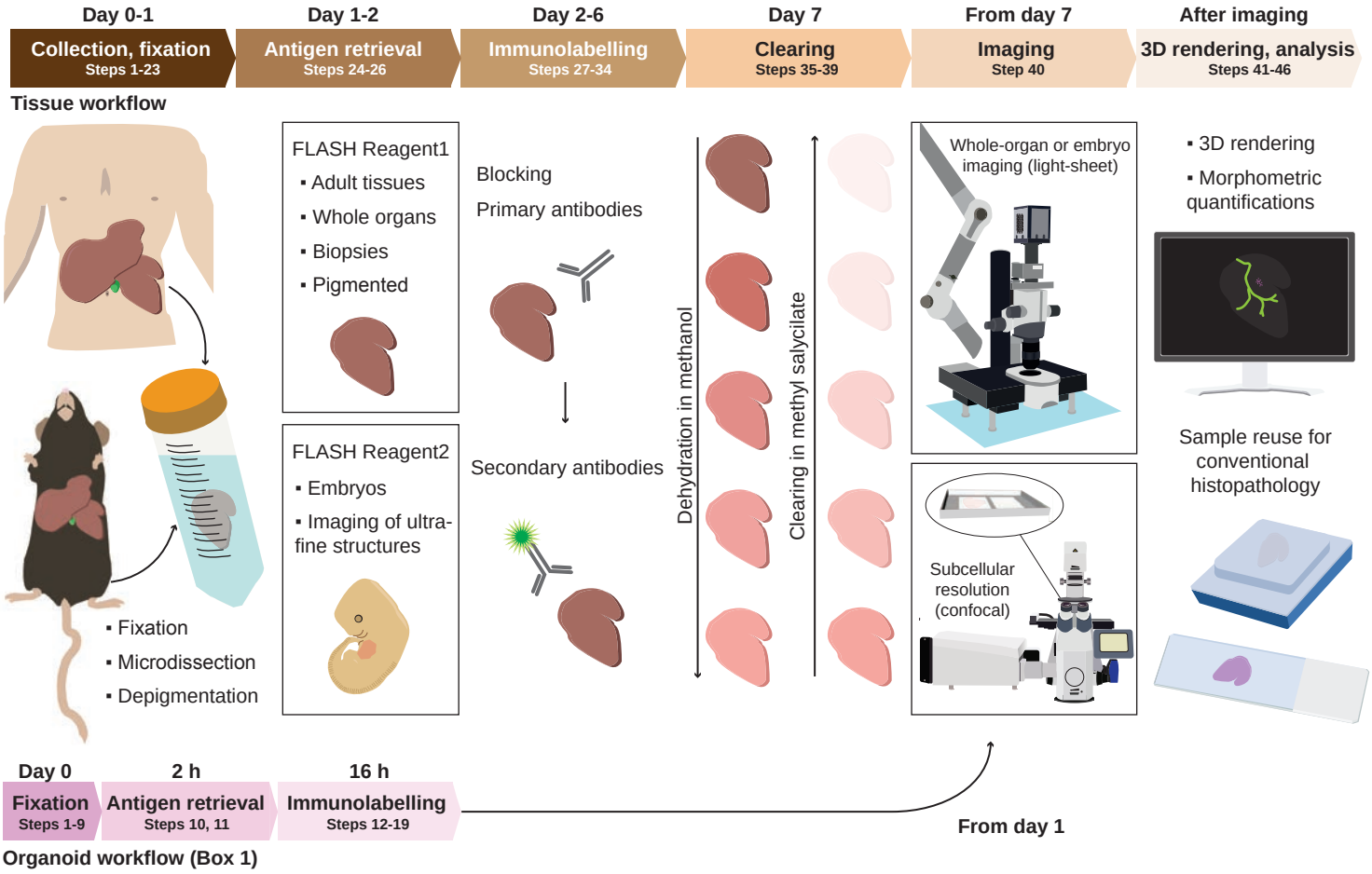
Day 0-1
Collection, fixation
Steps 1-23
Day 1-2
Antigen retrieval
Steps 24-26
Day 2-6
Immunolabelling
Steps 27-34
Day 7
Clearing
Steps 35-39
From day 7
Imaging
Step 40
After imaging
3D rendering, analysis
Steps 41-46
Tissue workflow
FLASH Reagent1
▪ Adult tissues
▪ Whole organs
▪ Biopsies
▪ Pigmented
FLASH Reagent2
▪ Embryos
▪ Imaging of ultra-fine structures
Blocking
Primary antibodies
Secondary antibodies
Dehydration in methanol
Clearing in methyl salycilate
Whole-organ or embryo imaging (light-sheet)
Subcellular resolution (confocal)
▪ 3D rendering
▪ Morphometric quantifications
Sample reuse for conventional histopathology
▪ Fixation
▪ Microdissection
▪ Depigmentation
Day 0
Fixation
Steps 1-9
2 h
Antigen retrieval
Steps 10, 11
16 h
Immunolabelling
Steps 12-19
From day 1
Organoid workflow (Box 1)

Figure 2

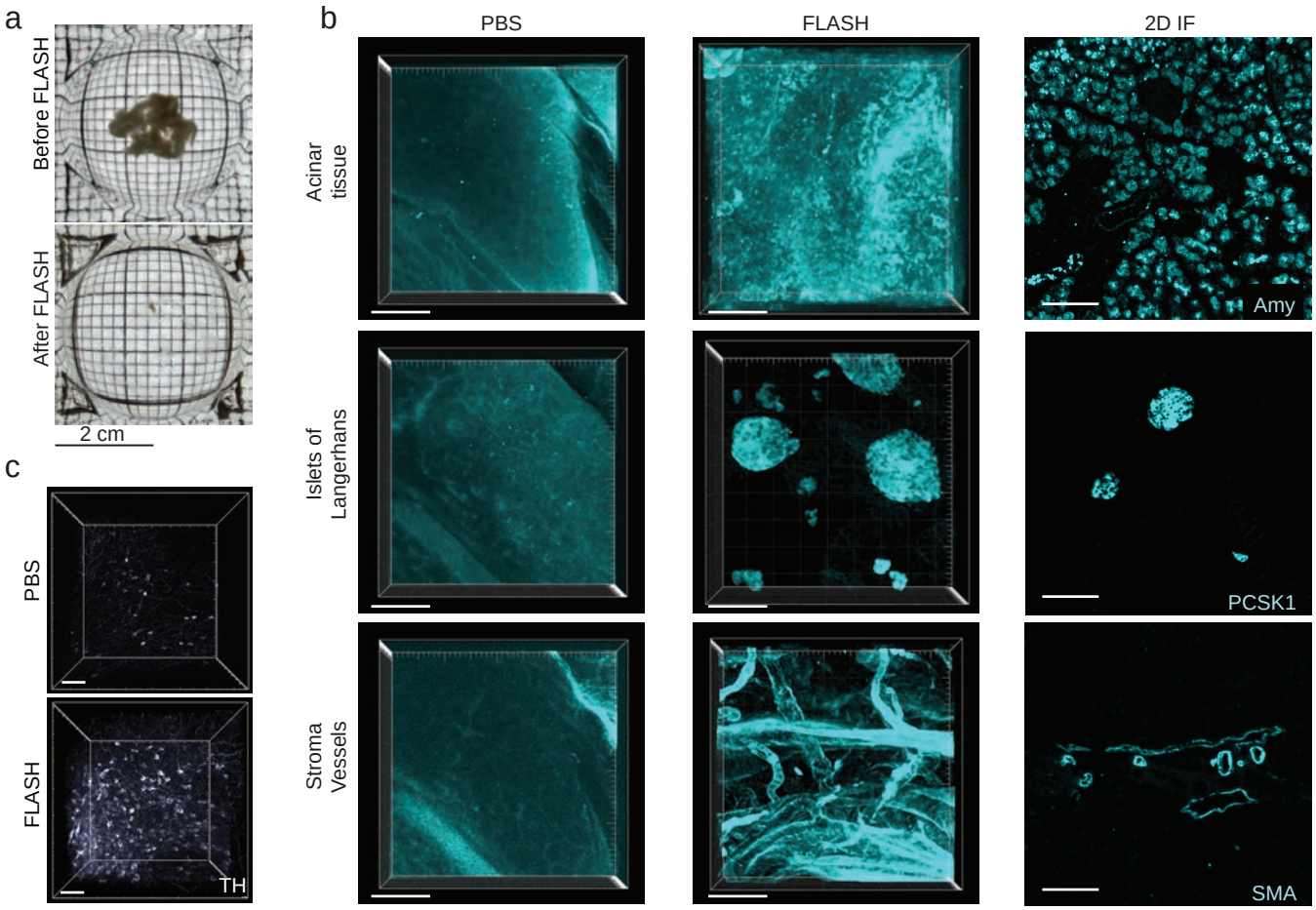
a
Before FLASH
After FLASH
2 cm
b
PBS
FLASH
2D IF
Acinar tissue
Islets of Langerhans
Stroma Vessels
Amy
PCSK1
SMA
c
PBS
FLASH
TH
d
Pancreas
e
Liver
f
Lung
After PBS
After FLASH

Figure 3

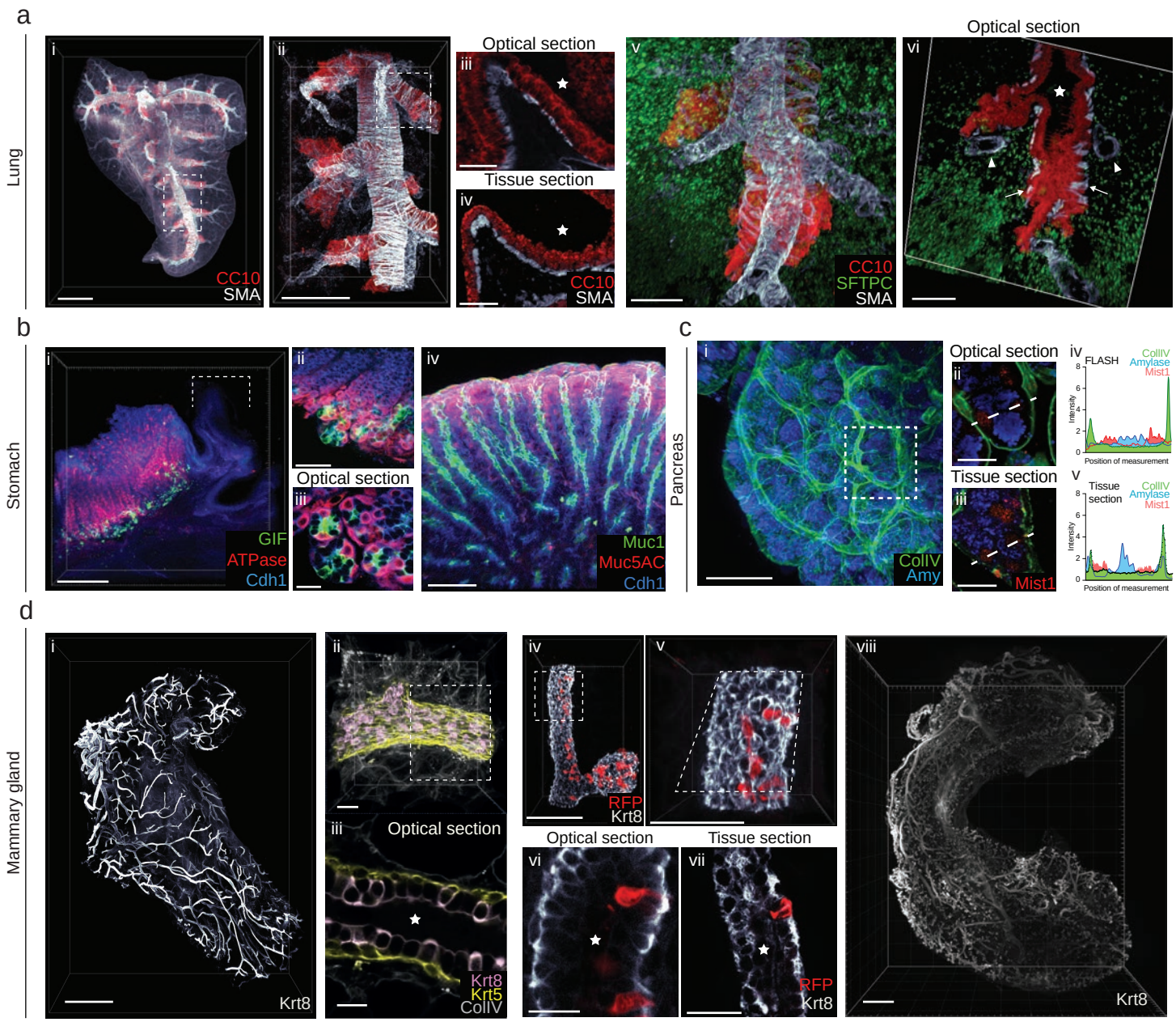
a
Lung
i
CC10
SMA
ii
Optical section
iii
Tissue section
iv
CC10
SMA
v
CC10
SFTPC
SMA
Optical section
vi
b
Stomach
i
GIF
ATPase
Cdh1
ii
Optical section
iii
iv
Muc1
Muc5AC
Cdh1
c
Pancreas
i
CollV
Amy
Optical section
ii
Tissue section
iii
Mist1
iv
FLASH
CollV
Amylase
Mist1
Intensity
Position of measurement
v
Tissue section
CollV
Amylase
Mist1
Intensity
Position of measurement
d
Mammary gland
i
Krt8
ii
iii
Optical section
Krt8
Krt5
CollV
iv
RFP
Krt8
v
Optical section
Tissue section
vi
vii
RFP
Krt8
viii
Krt8

Figure 4

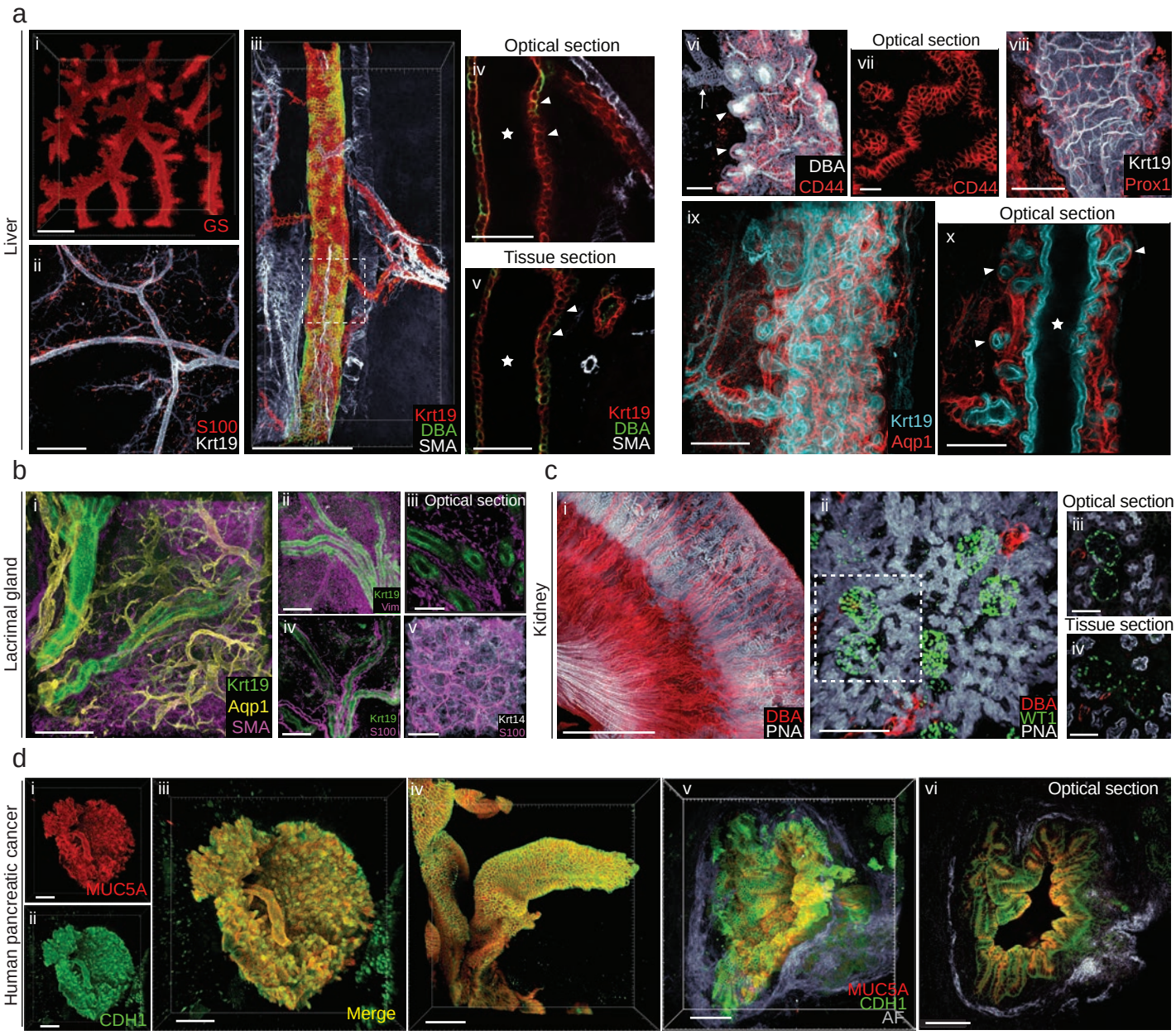
a
Liver
i
GS
ii
S100
Krt19
iii
Krt19
DBA
SMA
Optical section
iv
Tissue section
v
Krt19
DBA
SMA
vi
DBA
CD44
Optical section
vii
CD44
viii
Krt19
Prox1
ix
Krt19
Aqp1
Optical section
x
b
Lacrimal gland
i
Krt19
Aqp1
SMA
ii
Krt19
Vim
iii Optical section
iv
Krt19
S100
v
Krt14
S100
c
Kidney
i
DBA
PNA
ii
DBA
WT1
PNA
Optical section
iii
Tissue section
iv
d
Human pancreatic cancer
i
MUC5A
ii
CDH1
iii
Merge
iv
v
MUC5A
CDH1
AF
vi
Optical section

Figure 5

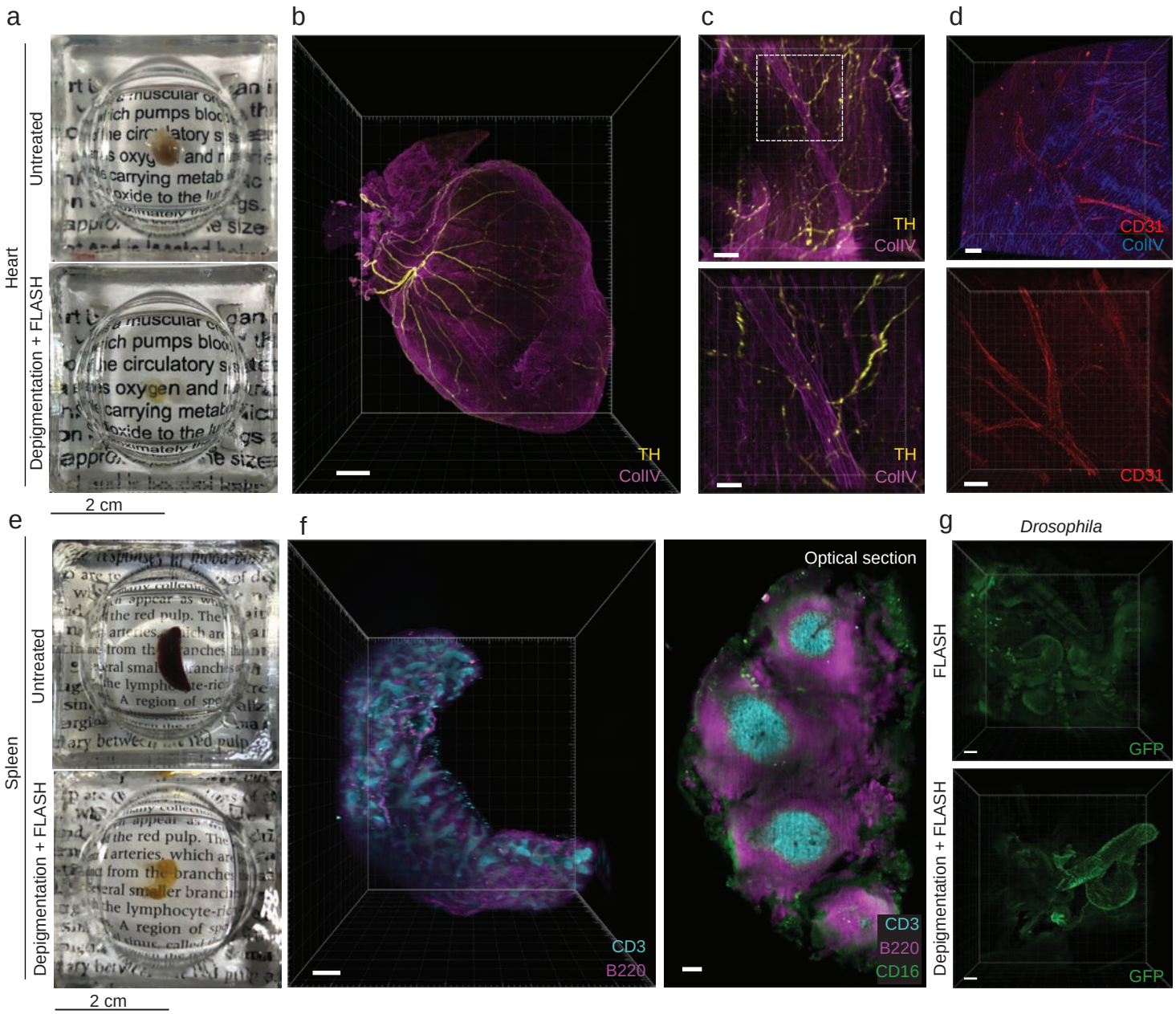
a
b
c
d
Heart
Untreated
Depigmentation + FLASH
2 cm
TH
ColIV
CD31
e
f
g
Spleen
Optical section
CD3
B220
CD16
Drosophila
FLASH
GFP

Figure 6

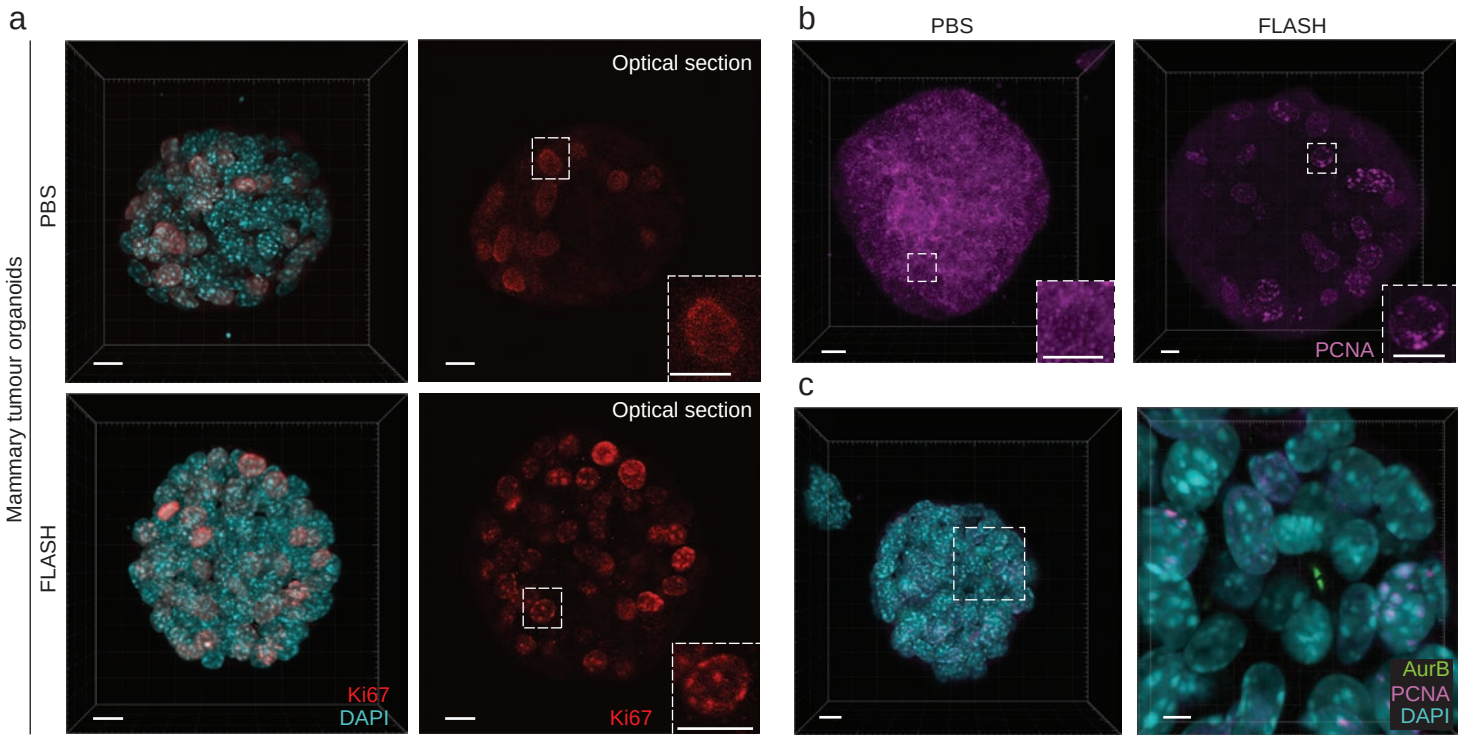
a
Mammary tumour organoids
PBS
FLASH
Optical section
Optical section
Ki67
DAPI
Ki67
b
PBS
FLASH
PCNA
c
AurB
PCNA
DAPI

Figure 7

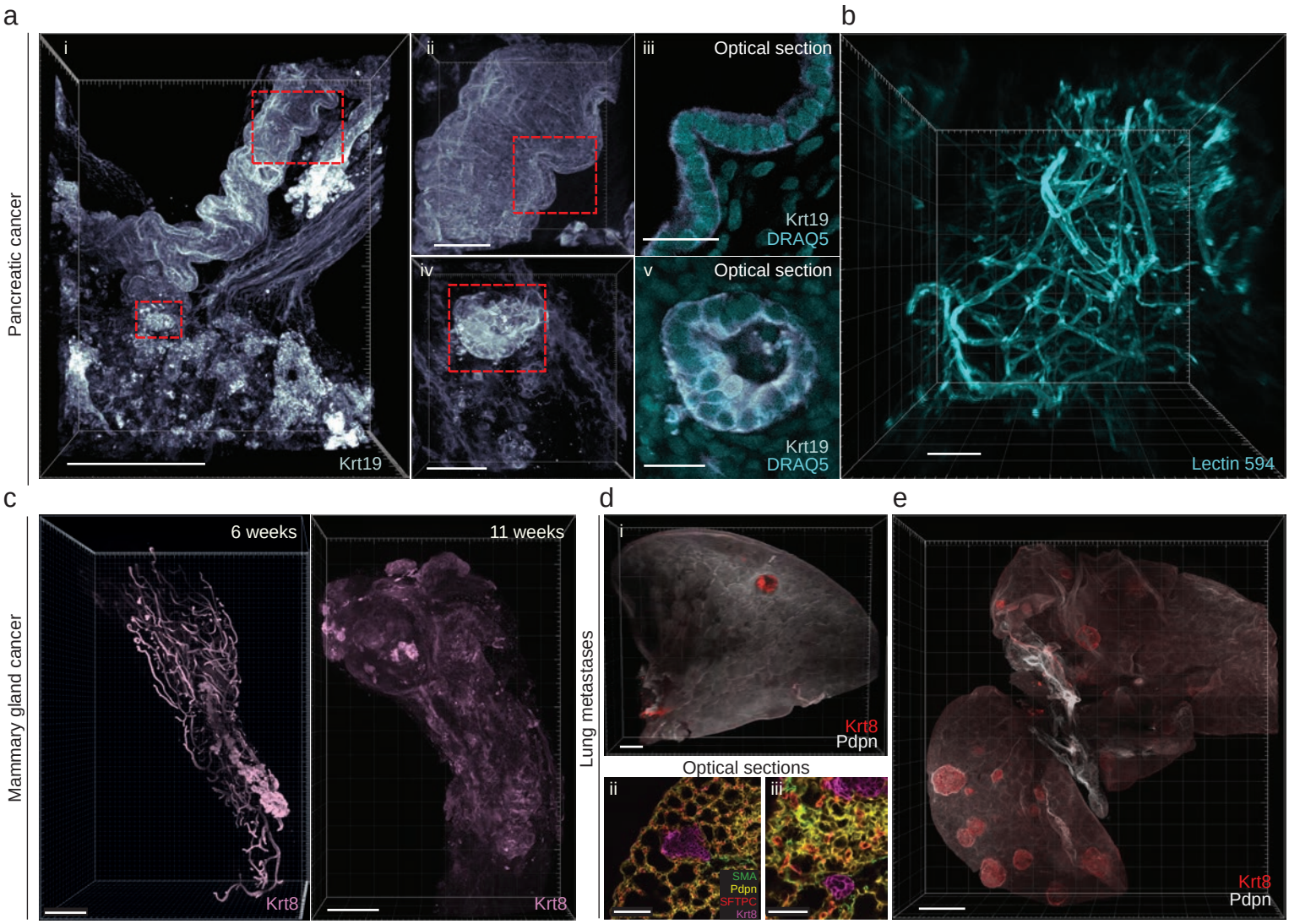
a
b
Pancreatic cancer
i
Krt19
ii
iii
Optical section
Krt19
DRAQ5
iv
v
Optical section
Krt19
DRAQ5
Lectin 594
c
d
e
Mammary gland cancer
6 weeks
Krt8
11 weeks
Krt8
Lung metastases
i
Krt8
Pdpn
Optical sections
ii
SMA
Pdpn
SFTPC
Krt8
iii
Krt8
Pdpn

Figure 8

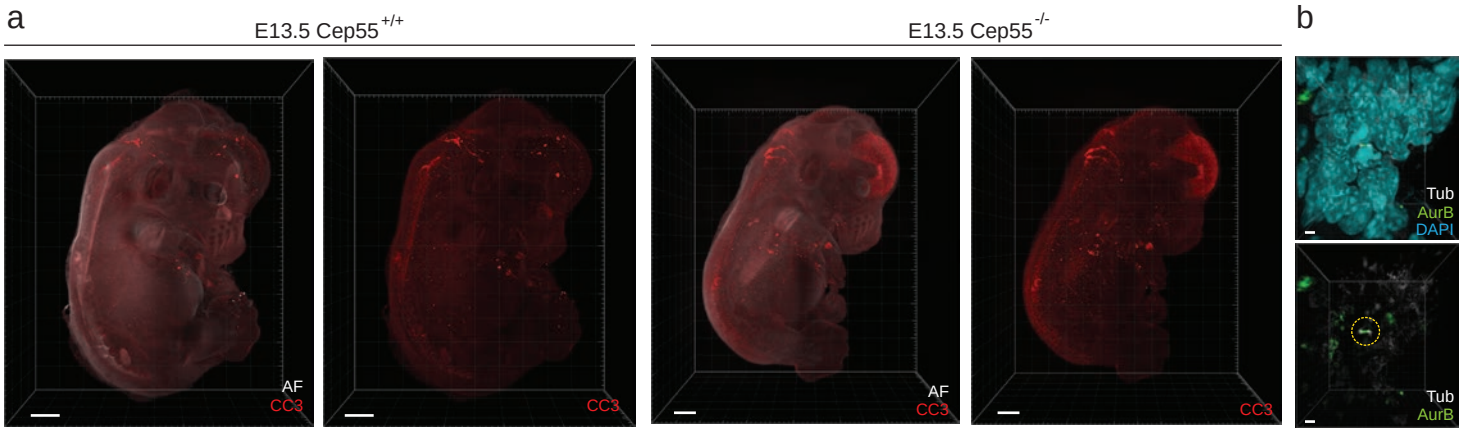
a
E13.5 Cep55+/+
E13.5 Cep55-/-
b
AF
CC3
CC3
AF
CC3
CC3
Tub
AurB
DAPI
Tub
AurB

Extended Data Figure 1

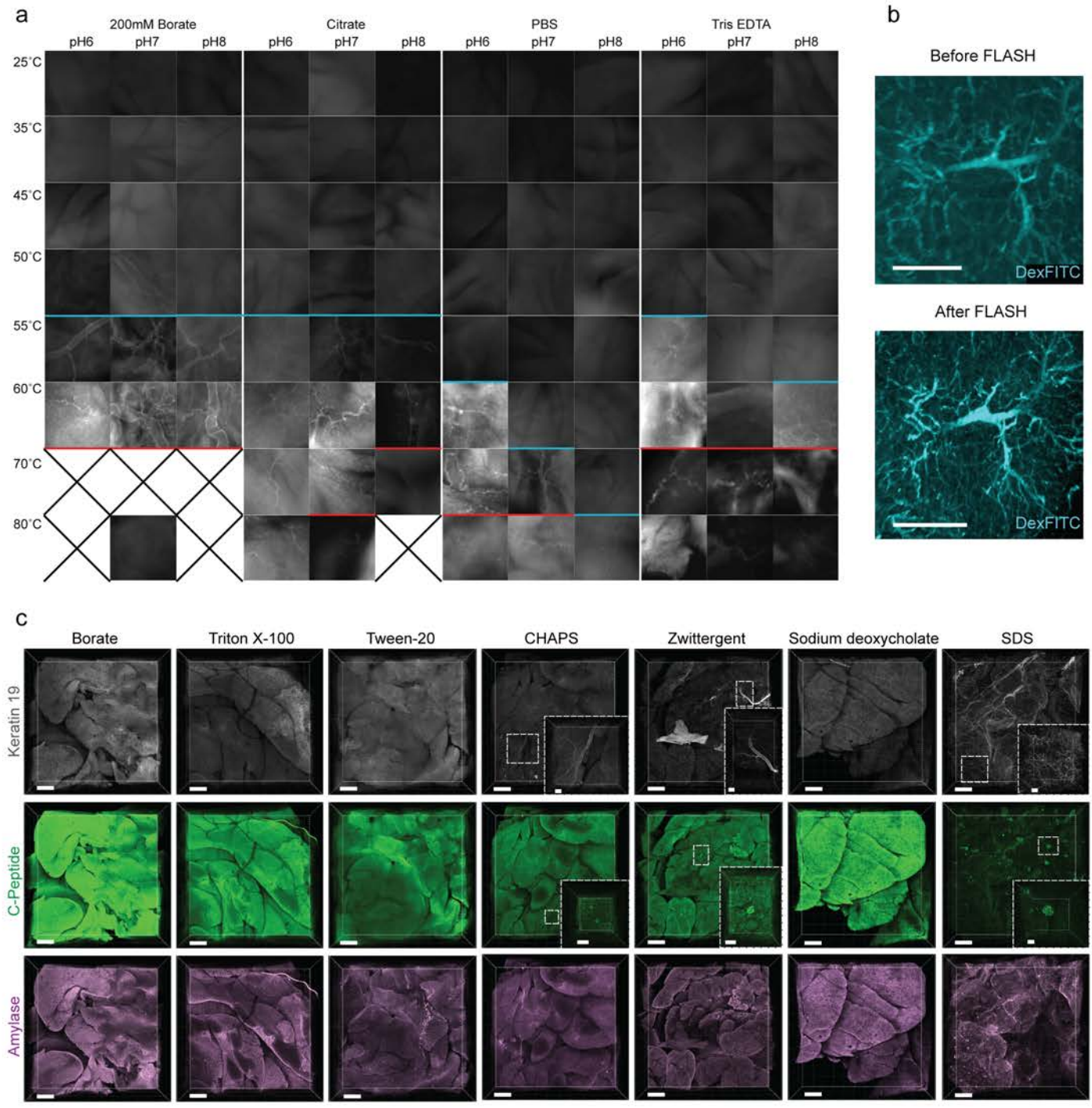

Extended Data Figure 2

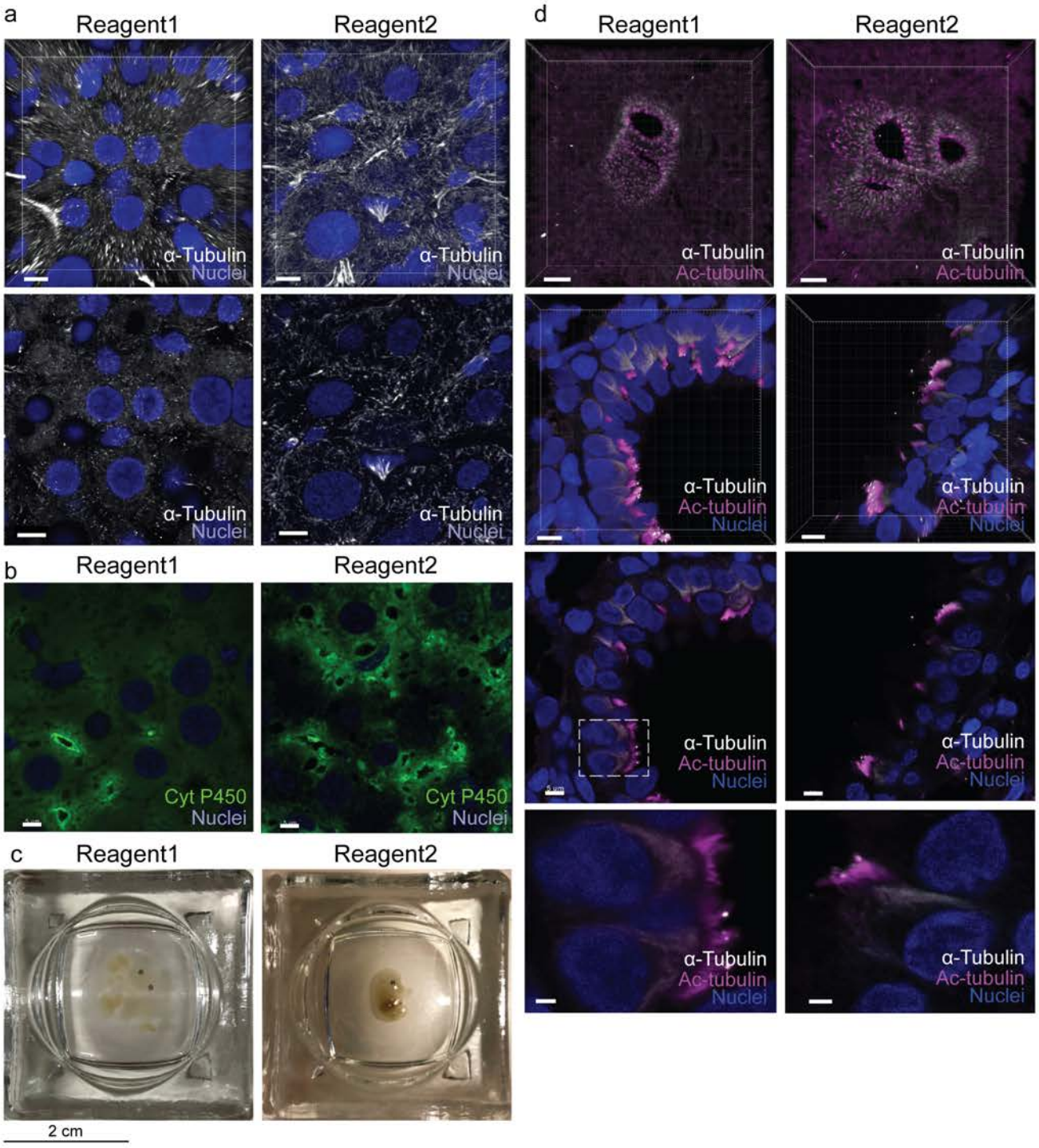

Extended Data Figure 3

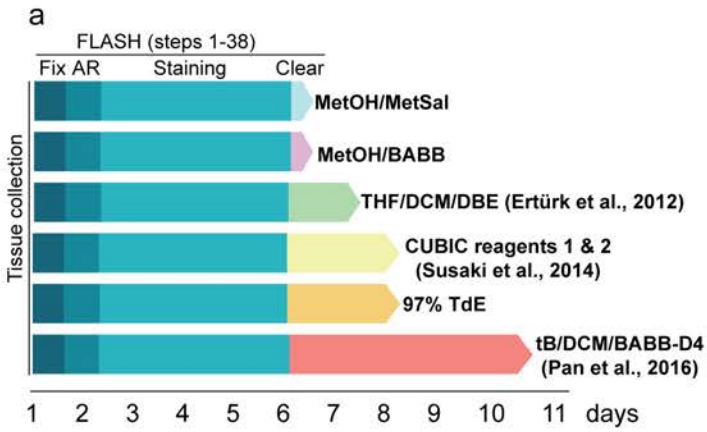

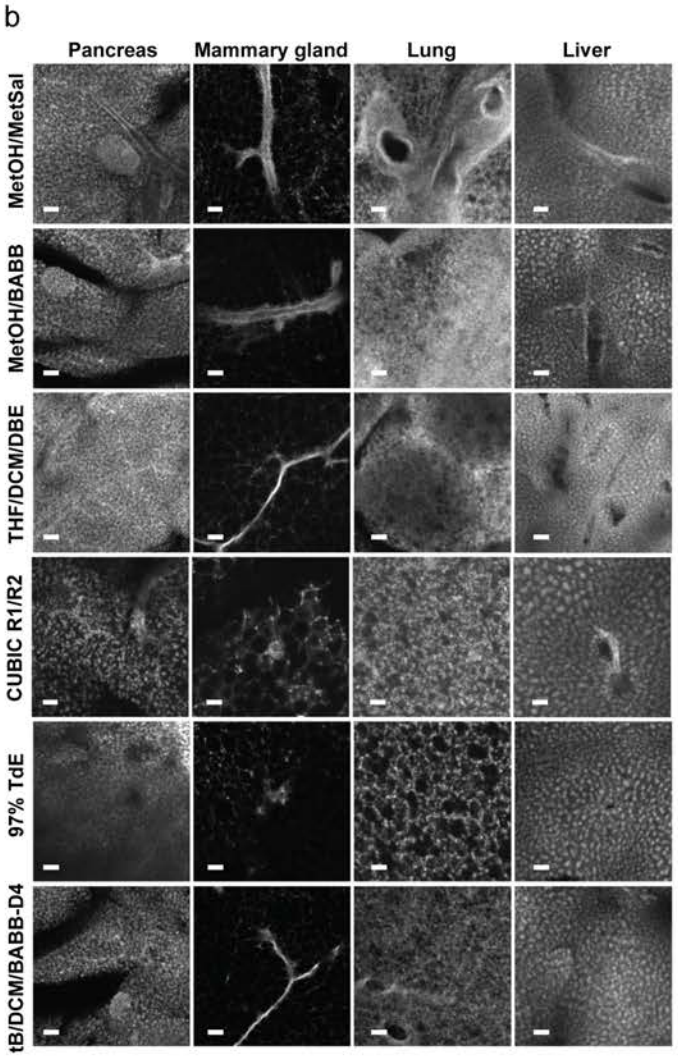

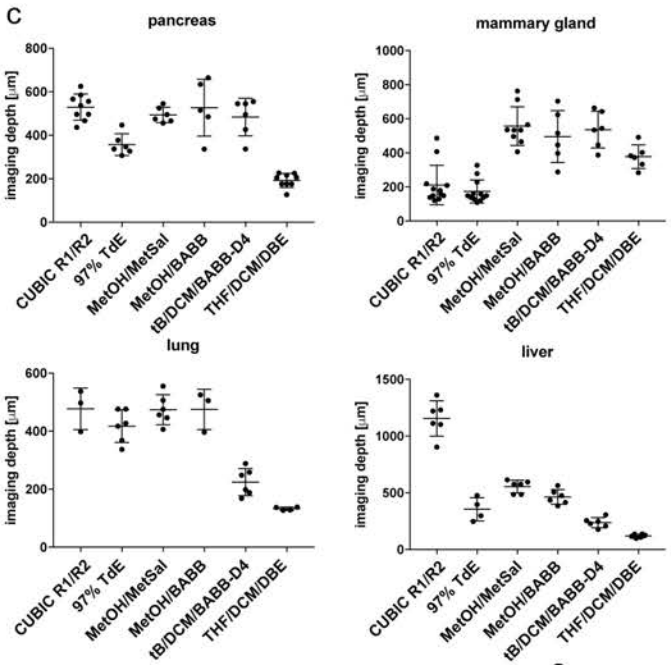

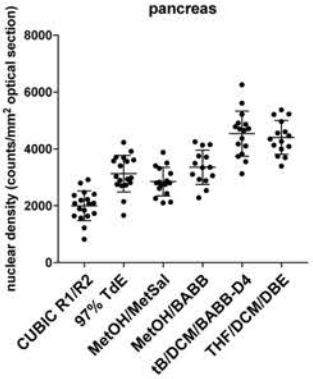

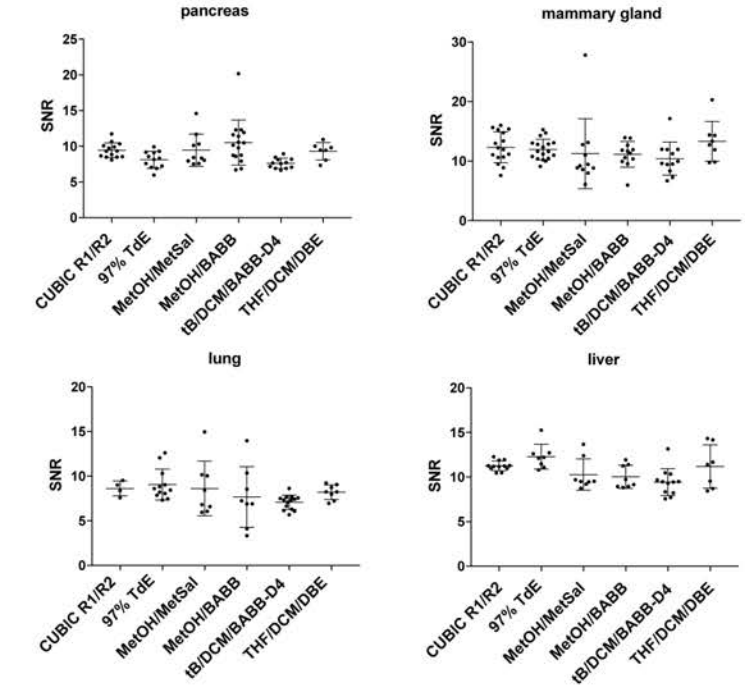

f

Media	RI
CUBIC R1/R2	1.46
97% TdE	1.52
MetOH/MetSal	1.536
MetOH/BABB	1.559
tB/DCM/BABB-D4	1.559
THF/DCM/DBE	1.562

Extended Data Figure 4

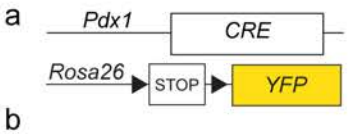

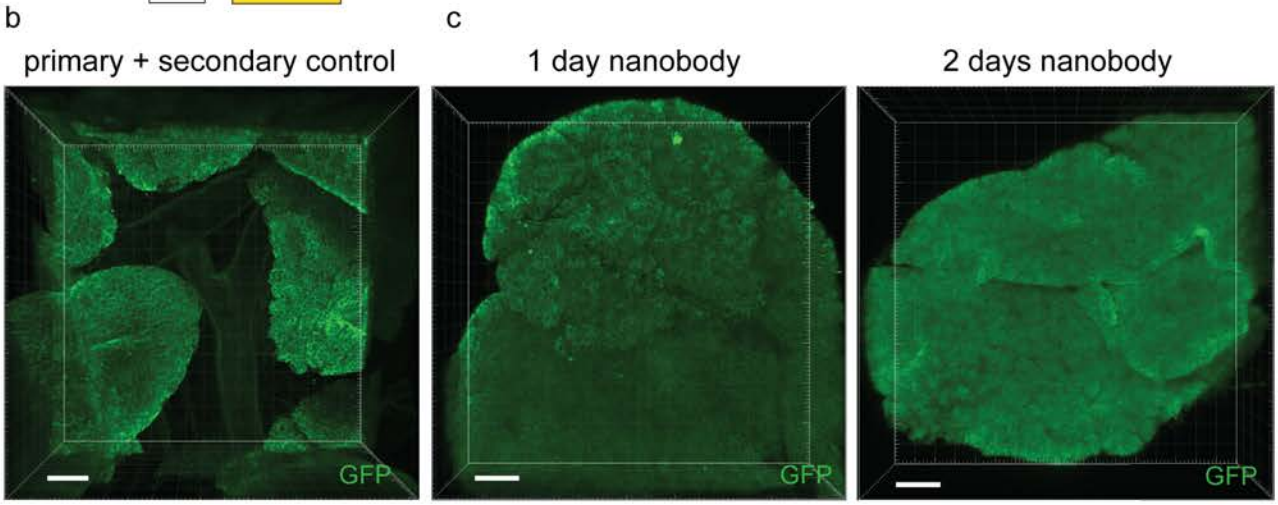

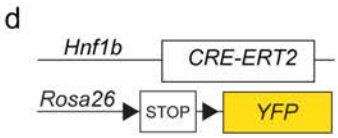

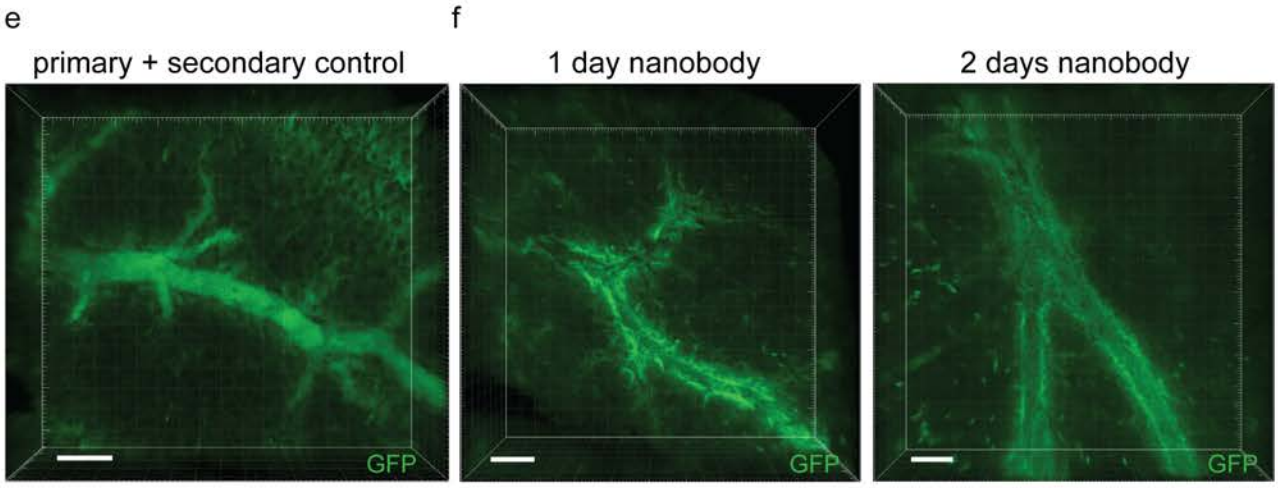

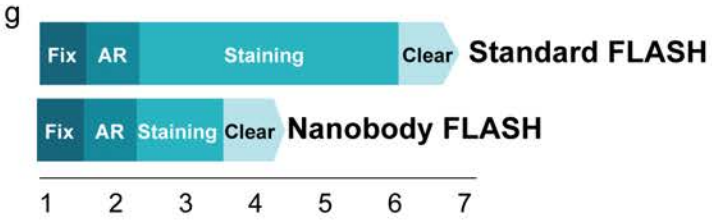

Extended Data Figure 5

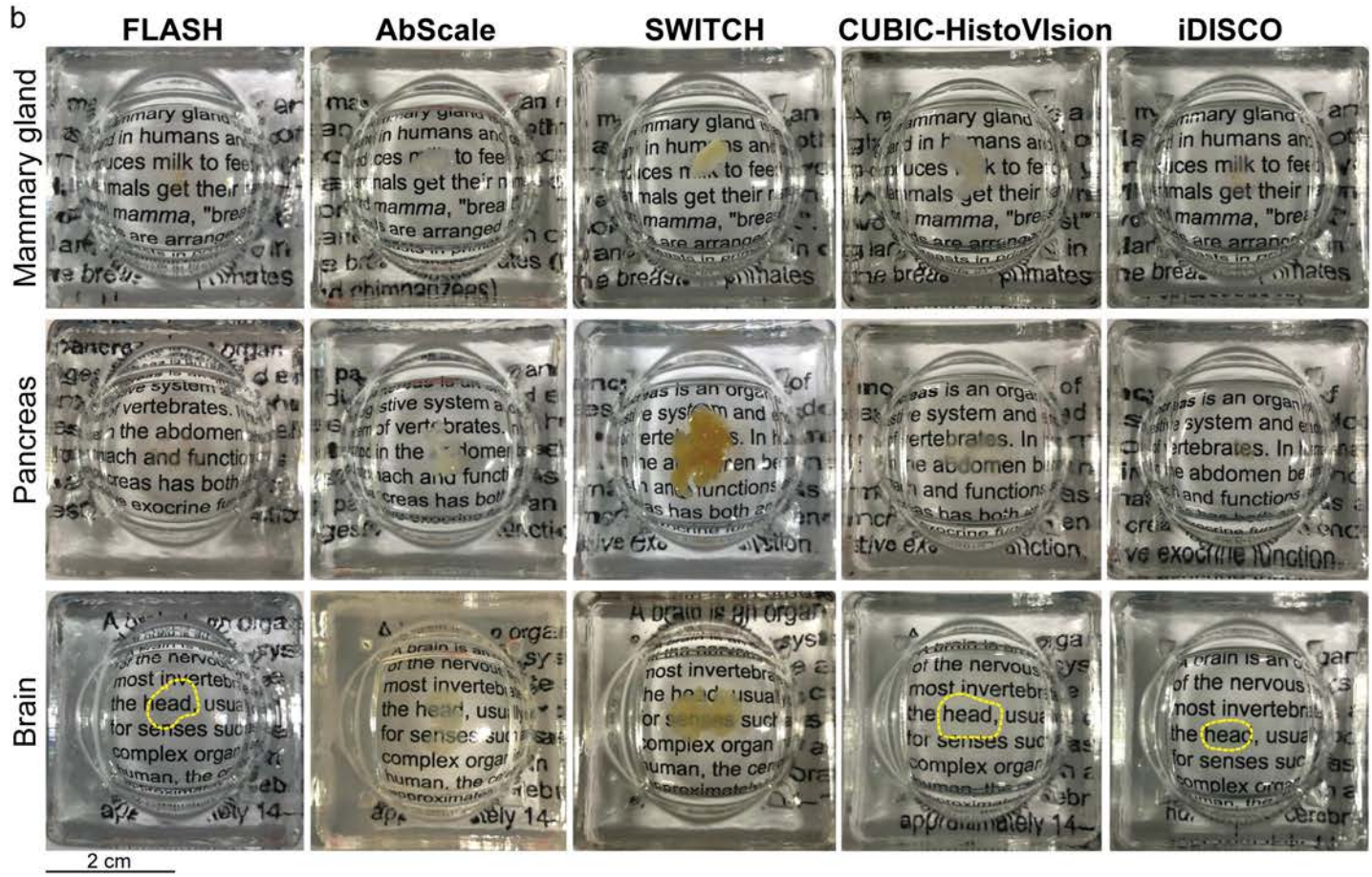

Extended Data Figure 6

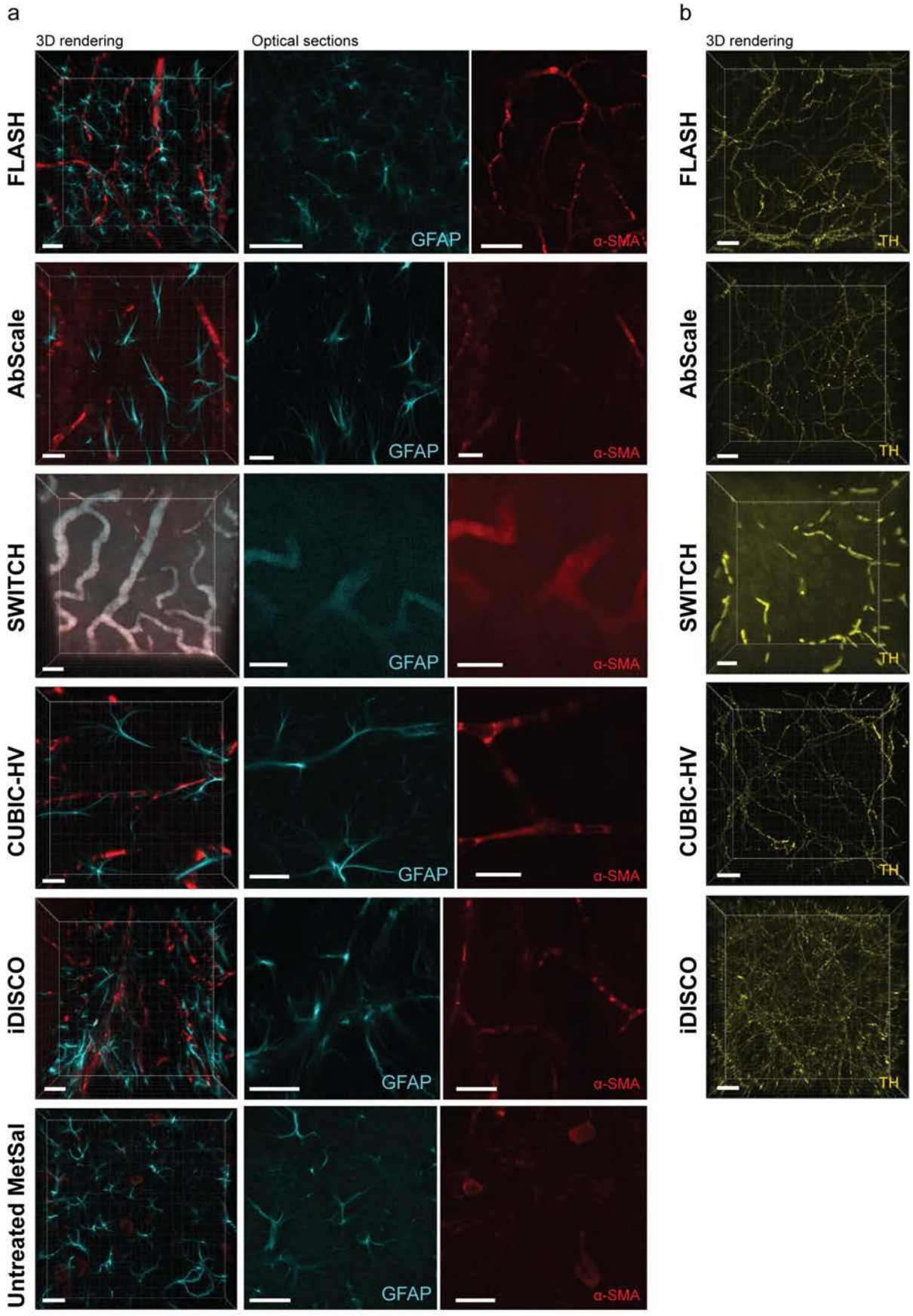

Extended Data Figure 7

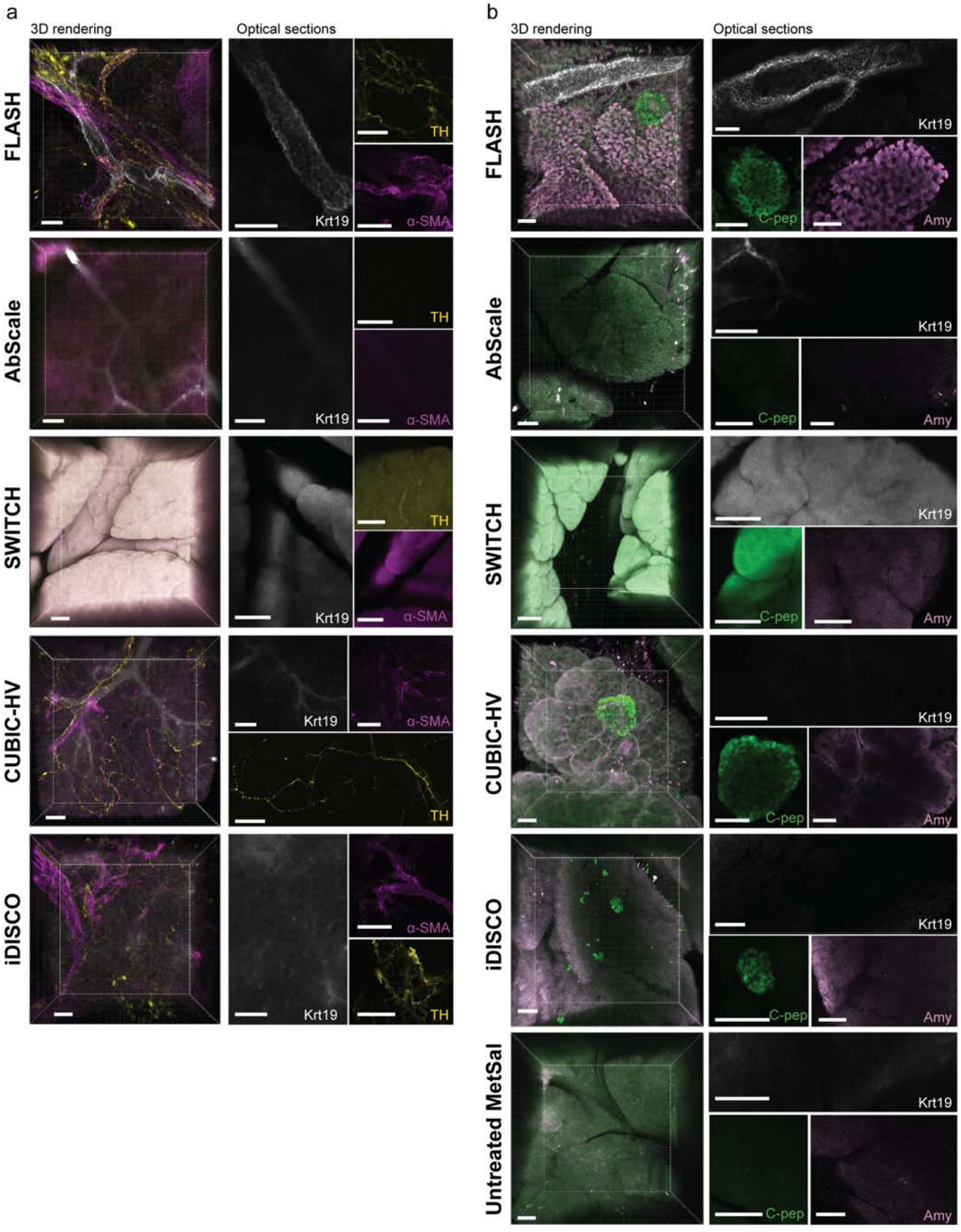

Extended Data Figure 8

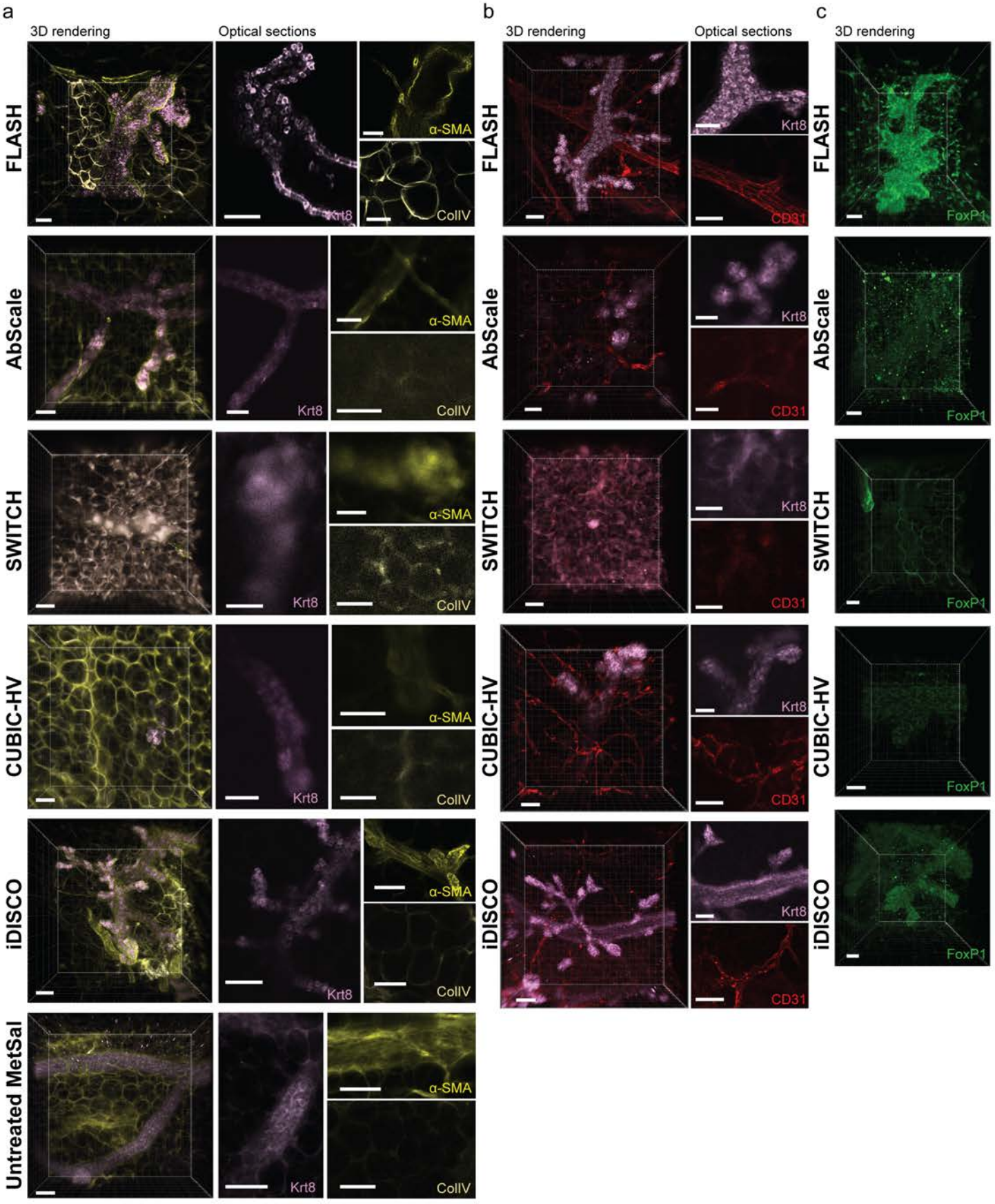

Extended Data Figure 9